The benefits of hierarchical ecosystem models: demonstration using a new state-space mass-balance model EcoState

Running title: Benefits of hierarchical ecosystem model

James T. Thorson[1,*], Kasper Kristensen[2], Kerim H. Aydin[1], Sarah K. Gaichas[3], David G. Kimmel[4], Elizabeth A. McHuron[5], Jens M. Nielsen[4,5], Howard Townsend[6], George A. Whitehouse[1,5]

[1] Resource Ecology and Fisheries Management, Alaska Fisheries Science Center, National Marine Fisheries Service, NOAA

[2] Technical University of Denmark, Charlottenlund Slot Jægersborg Allé 1, 2920 Charlottenlund, Denmark

[3] Ecosystem Dynamics and Assessment Branch, Northeast Fisheries Science Center, National Marine Fisheries Service, NOAA, 166 Water Street, Woods Hole, MA, USA

[4] Resource Assessment and Conservation Engineering, Alaska Fisheries Science Center, National Marine Fisheries Service, NOAA

[5] Cooperative Institute for Climate, Ocean, and Ecosystem Studies, University of Washington, Seattle, WA, USA

[6] Marine Ecosystems Division, Office of Science and Technology, National Marine Fisheries Service, Silver Spring, MD, United States

* Corresponding author: James.Thorson@noaa.gov

Abstract:

Ecosystem models predict changes in productivity and status for multiple species, and are important for incorporating climate-linked dynamics in ecosystem-based fisheries management. However, fishery regulations are primarily informed by single-species stock assessment models, which estimate unexplained variation in dynamics (e.g., recruitment, survival, fishery selectivity, etc) using random effects. We review the general benefits of estimating random effects in ecosystem models: (1) better representing biomass cycles and trends for focal species; (2) conditioning interactions upon observed biomass for predators and prey; (3) easier replication of model results using formal estimation rather than informal model "tuning;" (4) attributing process errors via comparison among different models. We then demonstrate these by introducing a new state-space model EcoState (and associated R-package) that extends mass-balance dynamics from Ecopath with Ecosim. This model estimates mass-balance (Ecopath) and time-dynamics (Ecosim) parameters dynamics directly via their fit to time-series data (biomass indices and fisheries catches) while also estimating the magnitude of process errors using RTMB. A real-world application involving Alaska pollock (*Gadus chalcogrammus*) in the eastern Bering Sea suggests that fluctuations in krill consumption are associated with cycles of increased and decreased pollock production. A self-test simulation experiment confirms that estimating process errors can improve estimates of productivity (growth and mortality) rates. Overall, we show that state-space mass-balance models can be fitted to time-series data (similar to surplus production stock assessment models), and can attribute time-varying productivity to both bottom-up and top-down drivers including the contribution of individual predator and prey interactions.

Keywords: Ecopath with Ecosim; state-space model; process errors; eastern Bering Sea; Alaska pollock; mass-balance model

Introduction

Throughout ecology and fisheries, there is broad agreement that model predictions often differ from real-world observations, and growing recognition that this discrepancy can be decomposed into measurement, process, and specification errors using hierarchical (a.k.a., mixed-effect or state-space) models. For example, hierarchical models are widely used in experimental analysis to account for pseudo-replication, comparative and life-history analysis to account for evolutionary similarity in model residuals (Felsenstein 1985), and population dynamics to account for unmodeled variation in demographic rates (de Valpine 2002). Hierarchical models for dynamics over time ("state-space models") specify a simplified model for system dynamics that typically involves one or more unknown parameter ("fixed effects"), and also estimate process errors that represent how dynamics differ from this parametric model. Process errors ("random effects") are then shrunk towards a shared mean, where the variance of these process errors can be estimated as a parameter and controls the magnitude of shrinkage (Thorson and Minto 2015).

Despite broad recognition about the importance of hierarchical modelling, they see surprisingly little use in marine ecosystem analysis. Ecosystem-based fisheries management (EBFM) has been adopted as a policy goal for ocean management agencies worldwide (FAO 2003; European Commission 2013; NOAA 2016), and ecosystem models are an essential tool for evaluating tradeoffs among alternative management scenarios within EBFM. Ecosystem models generally aim to represent changes in productivity and biomass for ecosystem components via trophic, technical, or other interactions (Hollowed et al. 2000). There are many types of ecosystem models with widely used software including (to name a few) Atlantis (Fulton et al. 2011), Ecopath with Ecosim (EwE), Mizer (Scott et al. 2014), Gadget (Begley and Howell

2004), and custom-built MICE models (Plagányi et al. 2014). Each model (and associated software) typically has different tools to "tune" parameters to improve fit to available data. For example, EwE involves a two-stage approach, where mass-balance is first achieved using Ecopath and then nonequilibrium dynamics are then projected over time using Ecosim. Ecosim vulnerability parameters are sometimes tuned via fit to predator-prey time-series (Scott et al. 2016; Bentley et al. 2024). However, time-series predictions of biomass are only calculated when tuning Ecosim (not when balancing the model in Ecopath), so this two-stage approach precludes using time-series data to tune the mass-balance parameters in Ecopath. Similarly, both Mizer and Gadget can estimate parameters representing ecosystem dynamics (Begley and Howell 2004; Spence et al. 2016). Although Mizer was later extended to estimate process errors (Spence et al. 2021), this has not been done for other major classes of ecosystem models.

In contrast to the dearth of hierarchical modelling for marine ecosystems, there is ongoing research to estimate time-varying parameters within single-species stock assessments using mixed-effect models (de Valpine 2002; Nielsen and Berg 2014). Stock assessments increasingly use state-space modelling (Stock and Miller 2021), and it is viewed as an essential feature for future assessment-model development (Punt et al. 2020). This increased use arises in part because state-space models can mitigate the bias that otherwise results from treating some time-varying process as if it was stationary in time (Xu et al. 2020; Stock et al. 2021). Importantly, random effects can also be used to represent systematic deviations away from the parametric model, and therefore represent "mis-specification error". In some cases, the magnitude of "mis-specification error" can be identified by estimating a new functional form for a modeled process using random effects (Thorson et al. 2014), while in other cases the "process error" represents nonstationarity over time in some model parameter. In either case, estimating

97 random effects allows an analyst to then expand the model and quantify how much the variance
98 of process errors is reduced by a given model development. In this interpretation, process errors
99 allow analysts to attribute unmodeled variation to specific hypothesized drivers.
100 We propose that hierarchical models will provide several benefits for ecosystem models,
101 and deserve adoption across the full range of ecosystem-model software. These benefits include:
102 1. Better representing biomass cycles and trends for focal species, i.e., where population
103 dynamics for individual species may be driven by physical variables or interactions that are
104 not easy to represent explicitly, but whose effect is evident in available time-series.
105 Hierarchical models can then represent these patterns as process errors, and thereby capture
106 apparent patterns in stock status. This model behavior is similar to the treatment of
107 recruitment-deviations in stock assessment, and it would allow ecosystem models to be used
108 to measure stock status and trends;
109 2. Conditioning interactions upon observed biomass for predators and prey, i.e., where trends or
110 cycles in biomass for dominant predator or forage species (which might not be represented
111 without process errors) can then be propagated through ecosystem interactions. Hierarchical
112 models would therefore ensure that predator consumption or forage availability matches
113 observed patterns, and that resulting predictions of species interactions are then accurately
114 represented for other modeled taxa;
115 3. Easier replication of model results using formal estimation rather than informal model
116 tuning, i.e., where models can be fitted using a statistical optimizer rather than using “forcing
117 functions” or ad hoc model changes. By using a statistical optimizer, hierarchical models
118 then guarantee that any analyst will arrive at the same model for a given set of data and

model assumptions. This then allows the model to be updated over time by new analysts, or replicated independently;

4. Attributing observed patterns to alternative mechanistic drivers, i.e., where the analyst then seeks to identify changes in model structure that can reduce the magnitude of estimated process errors. These changes might include (A) attributing patterns to hypothesized oceanographic or ecological mechanisms that are measured as covariates, and/or (B) adding new mechanisms and functional groups to the model. Hierarchical modelling helps by allowing models to be rapidly refitted using statistical optimization, and also allows statistical comparison among alternative models.

These benefits are generally observed in the relatively few ecosystem models that include process errors (Spence et al. 2021), but have not explored for the wide range of ecosystem models.

To demonstrate these benefits, we introduce a new state-space mass-balance model that incorporates both top-down and bottom-up interactions. Using a case study representing the eastern Bering Sea centered on prey, competitors, and predators for Alaska pollock (*Gadus chalcogrammus*), we demonstrate that estimating process errors improves ecological inference and expected statistical performance. Specifically, biomass cycles for krill are associated with cycles of higher or lower productivity (and resulting biomass) for pollock, and these apparent decadal cycles are not captured without estimating process errors. We also use a simulation experiment to confirm that estimating process errors results in more accurate and precise estimates of growth and mortality rates than ignoring process errors, and that known parameter values can be recovered with reasonable precision. Finally, we conclude by discussing how

hierarchical ecosystem models might mitigate capacity constraints that hamper wider adoption and tactical application of ecosystem models.

Methods

We demonstrate the general utility of hierarchical modelling for ecosystem analysis by introducing an extension of Ecopath with Ecosim that estimates both parametric uncertainty and the variance of residual variation in biomass dynamics ("process errors"). The associated R-package EcoState uses RTMB (Kristensen 2024a) to implement automatic differentiation and fit process errors via maximum marginal likelihood. Our demonstration is intended in part to demonstrate that automatic differentiation and the Laplace approximation (via RTMB) can be used to fit nonlinear ordinary differential equations with many variables, as required for many ecosystem models. Parametric uncertainty and process errors have been added previously to other ecosystem models, e.g., Mizer (Spence et al. 2016, 2021), but EwE has typically separated mass balance (Ecopath) from biomass projections (Ecosim) and therefore precluded estimating mass-balance parameters using time-series data. EcoState is therefore the first (to our knowledge) model to formally estimate mass-balance and process-error parameters using a mass balance dynamics, and mass-balance provides an avenue to incorporate bottom-up dynamics (i.e., where prey availability affects predator productivity).

Benefits of hierarchical modelling for mass-balance ecosystem models

EcoState demonstrates the advantages of hierarchical ecosystem modelling relative to previous mass-balance models (Christensen and Walters 2004; Lucey et al. 2020) in several ways:

1. *Joint modelling*: It combines the mass-balance done by Ecopath with the dynamical projection from Ecosim within a single statistical model. It therefore replaces a 2-stage workflow with a single model, and allows the model to be easily refitted (including

rebalancing the population scale) when adding/dropping taxa or data. This involves estimating equilibrium population biomass, nonequilibrium initial conditions, catchability coefficients, the variance of process errors via fit to available time-series, as well as predator-prey vulnerability, production, and consumption per biomass. Ecosim has previously been fitted to estimate vulnerability parameters using likelihood or sum-of-squares methods (Gaichas et al. 2012; Scott et al. 2016; Bentley et al. 2024), but we do not know of efforts to jointly estimate mass-balance (Ecopath) and vulnerability (Ecosim) parameters;

2. *Process errors*: By estimating process errors, we ensure that estimated mass $\beta_{s,t}$ is shrunk towards measured values $q_s b_{s,t}$ whenever measurements are available. This then ensures that modeled consumption is shrunk towards the quantity expected given that measured mass, i.e., that systematically over- or underestimating mass for a variable relative to observations does not propagate into over- or under-estimated consumption for interacting species. For variables that have no biomass measurements, dynamics are then inferred based on time-varying productivity resulting from changes in modeled consumption (and resulting gain and loss rates) conditional upon those estimated process errors;
3. *Model bridging*: If the analyst chooses to specify all parameters and turn off process errors, then dynamics will be similar to those from Ecopath and Ecosim. This then facilitates model building, i.e., by starting with published EwE models and progressively "turning on" different parameters and/or process errors;
4. *Forecast variance*: If the analyst chooses to model future years with no available data regarding absolute or relative mass, they must still specify a value for catch in those future years. Having done this, the model will automatically propagate uncertainty about process errors $\boldsymbol{\epsilon}(t)$ and resulting uncertainty about biomass $\boldsymbol{\beta}(t)$ in those future years;

5. *Exploring ecosystem modules*: Finally, the analyst may want to isolate interactions among a small subset of taxa ("species module;" Holt 1997). The model still estimates consumption among those taxa that are retained, but typically identifies decreased ecotrophic efficiency for those taxa whose predators are excluded. This addresses ongoing calls for "minimal realistic models," whether using mass-balance dynamics (Walters et al. 1997) or otherwise (Plagányi et al. 2014).

These features are common in modern stock assessment models, but novel for mass-balance ecosystem models.

Mass-balance based on Ecopath

EcoState is a mass-balance model that can be solved for equilibrium mass of different ecosystem components (e.g., detritus, primary producers, consumers, and predators) that are coupled via consumption, production, and detrital production/decomposition rates (Polovina 1984). EcoState tracks mass-vector $\boldsymbol{\beta}$ composed of mass β_s for each functional group or detrital pool (called "variables" in the following), indexed by $s \in \{1,2,\ldots,S\}$ where S is the total number of variables. Each variable is then specified as an (1) autotroph (i.e., primary producer), (2) heterotroph (i.e., consumer or predator), or (3) detritus. We attempt to use mathematical notation following guidelines from Edwards and Auger-Méthé (2019), particularly by using Greek letters for state-variables (e.g., biomass), Roman for parameters and data, vector-matrix notation (i.e., lowercase italic for scalars), and avoiding the use of multiple letters for a single parameter. This results in some departures from previous Ecopath and Ecosim notation (see Table S1 for a summary of all notation), although we use similar symbols where practical. We refer to the combination of autotrophs and heterotrophs as "biomass" or "taxa," and we also index variables as prey $i \in \{1,2,\ldots,S\}$ and predator $j \in \{1,2,\ldots,S\}$ in expressions where prey and predators are both

included. Each variable s at equilibrium is assumed to have a fixed ratio of production to biomass p_s, consumption to biomass w_s (where $w_s = \text{NA}$ for detritus and primary producers), and a fixed $S \times S$ diet matrix $\mathbf{D}$ containing the proportion $d_{i,j}$ of diet provided by each potential prey i for predator j (where $d_{i,j} = 0$ for detritus and primary producers as "predators" j and all "prey" i). Finally, each variable is assumed to have mass that is "used" in the system (i.e., consumed by predators or removed by fisheries), and this is represented as ecotrophic efficiency e_s.

Similar to Ecopath, equilibrium in EcoState occurs for each variable when its gain matches loss rate. To match notation that is common in stock-assessment models, we define equilibrium mass $\bar{\beta}_s$ as the average mass in the absence of fishing:

$$\underbrace{\bar{\beta}_i}_{\substack{\text{Equilibrium} \\ \text{biomass for prey i}}} \times \underbrace{p_i}_{\substack{\text{Prey} \\ \text{production} \\ \text{per biomass}}} \times \underbrace{e_i}_{\substack{\text{Prey} \\ \text{ecotrophic} \\ \text{efficiency}}} \tag{1}$$

$$= \sum_{j=1}^{S} \left(\underbrace{d_{i,j}}_{\substack{\text{Proportion of} \\ \text{diet for predator} \\ j \text{ by prey } i}} \times \underbrace{\bar{\beta}_j}_{\substack{\text{Equilibrium} \\ \text{biomass for} \\ \text{predator } j}} \times \underbrace{w_j}_{\substack{\text{Predator} \\ \text{consumption} \\ \text{per biomass}}} \right)$$

Later, we incorporate fishing mortality to project ecosystem dynamics away from this unfished equilibrium. Unknown values in Eq. 1 can be solved by re-expressing it in vector-matrix notation. Specifically, gains (left side of Eq. 1) are written as $\boldsymbol{\beta} \odot \mathbf{p} \odot \mathbf{e}$, where e.g. $\boldsymbol{\beta} \odot \mathbf{p}$ is the Hadamard (elementwise) product of two vectors $\boldsymbol{\beta}$ and $\mathbf{p}$. Similarly, losses (right side of Eq. 1) are s $\mathbf{D}(\boldsymbol{\beta} \odot \mathbf{w})$. Equilibrium biomass $\overline{\boldsymbol{\beta}}$ is achieved when these rates match, i.e. $\overline{\boldsymbol{\beta}} \odot \mathbf{p} \odot \mathbf{e} = \mathbf{D}(\overline{\boldsymbol{\beta}} \odot \mathbf{w})$, which can be solved for some combination of equilibrium biomass $\overline{\boldsymbol{\beta}}$ and

ecotrophic efficiency (Supplementary Materials 2). Given this equilibrium, we then calculate equilibrium consumption $\bar{\mathbf{C}}$:

$$\bar{\mathbf{C}} = \mathbf{D} \odot \left(\mathbf{1} \left(\bar{\boldsymbol{\beta}} \odot \mathbf{w} \right)^{\boldsymbol{T}} \right) \quad (2)$$

where $\mathbf{1}$ is a column-vector of 1s such that $\mathbf{1}\left(\bar{\boldsymbol{\beta}} \odot \mathbf{w}\right)^{T}$ is a matrix of equilibrium consumption $\bar{\boldsymbol{\beta}} \odot \mathbf{w}$ for each predator, repeated as separate rows for each prey.

The fitted model can then be used to solve for equilibrium levels of a specified tracer y_s for each taxon s. This tracer $\mathbf{y}$ represents any physical or theoretical quantity that is tracked as it progresses through the food chain via consumption under the expression $\mathbf{z} = \mathbf{z}\mathbf{C}^{*} + \mathbf{y}$ where $\mathbf{C}^{*}$ is the consumption $c_{i,j}$ for each prey i by each predator j rescaled to sum to one for each predator to represent a proportion, and $\mathbf{z}$ is the equilibrium concentration of a tracer to be estimated. For example, trophic level is defined as a tracer such that $\mathbf{z} = \mathbf{z}\mathbf{C}^{*} + \mathbf{y}$, where $\mathbf{y} = \mathbf{1}$ is the increase in trophic level each time mass is consumed. This simultaneous equation for trophic level is then solved as $\mathbf{z} = \mathbf{1}^{t}(\mathbf{I} - \mathbf{C}^{*})^{+}$, where $(\mathbf{I} - \mathbf{C}^{*})^{+}$ is the Penrose-Moore pseudoinverse of $\mathbf{I} - \mathbf{C}^{*}$ and $\mathbf{1}^{t}$ is a row-vector of 1s. Alternatively, we define tracer $\mathbf{y}$, e.g., as an indicator vector that is 1 for the base of the pelagic food chain and 0 otherwise, and then calculate the proportion of biomass for each taxon that results from pelagic production as $\mathbf{z} = \mathbf{y}^{T}(\mathbf{I} - \mathbf{C}^{*})^{+}$.

Time-dynamics based on Ecosim

After Ecopath is applied to achieve mass-balance for all species, Ecosim is separately used to simulate dynamics forward in time (Pauly et al. 2000; Christensen and Walters 2004). By contrast, EcoState uses proposed parameters to solve for missing values that achieve mass-balance, and simultaneously uses those parameters to project dynamics for all variables at times $t \in \{t_1, t_2, \ldots, T\}$ while integrating dynamics over the interval between these times (e.g., from t_1 to t_2). We discretize time into years in the following, but future research could incorporate

seasonal (e.g., monthly) variation using a higher-resolution time-interval with no change in equations or code. Similarly, future research could explore how fishing mortality affects the prey production p_i and predator consumption w_i via its impact on age-structure (Aydin 2004), although we do not do so here.

Adapting notation from Lucey et al. (2020), EcoState represents similar dynamics as Ecosim by specifying a differential equation for mass:

$$\frac{d}{dt}\boldsymbol{\beta}(t) = \left(\underbrace{\mathbf{g}(t)}_{\substack{\text{Growth} \\ \text{rate}}} - \underbrace{\mathbf{m}(t)}_{\substack{\text{Natural} \\ \text{mortality} \\ \text{rate}}} - \underbrace{\mathbf{f}(t)}_{\substack{\text{Fishing} \\ \text{mortality} \\ \text{rate}}} \right) \odot \boldsymbol{\beta}_t \tag{3}$$

where $f_s(t)$ is fishing mortality rate and both growth rate $g_s(t)$ and loss rate $m_s(t)$ are calculated from annual consumption rate $\mathbf{C}(t)$, representing the mass $c_{i,j}(t)$ of prey i consumed by predator j, where $\frac{d}{dt}\boldsymbol{\beta}(t) = \mathbf{0}$ whenever $\boldsymbol{\beta}_t = \overline{\boldsymbol{\beta}}$ in the absence of fishing. Future studies could include net migration, although this is often not considered in stock-assessment models and therefore ignored here as well. This equation also assumes that parameters in growth and natural mortality rates are stationary over time. Future studies could address ontogenic shifts in diet by incorporating stanzas (i.e., age-structured models for selected taxa), and could estimate time-varying diet or other parameters by fitting directly to diet time-series data. EcoState provides a general platform for these extensions, although we do not implement them here.

Consumption rate $\mathbf{C}(t)$ varies around equilibrium consumption $\bar{c}_{i,j}$ based on predator and prey mass:

$$c_{i,j}(t) = \underbrace{\bar{c}_{i,j}}_{\substack{\text{equilibrium} \\ \text{consumption rate}}} \times \frac{x_{i,j}\dfrac{\beta_j(t)}{\bar{\beta}_j}}{\underbrace{x_{i,j} - 1 + \dfrac{\beta_j(t)}{\bar{\beta}_j}}_{\substack{\text{predator functional} \\ \text{response}}}} \times \underbrace{\frac{\beta_i(t)}{\bar{\beta}_i}}_{\substack{\text{prey functional} \\ \text{response}}} \tag{4}$$

where **X** is the matrix of predator-prey vulnerability parameters containing the vulnerability $x_{i,j}$ for prey i to predator j (Aydin 2004 Eq. 1; Plagányi and Butterworth 2004). Our model for consumption (Eq. 4) does not include those processes that are eliminated using default values in EwE as implemented in the Rpath package (Lucey et al. 2020), and see Supplementary Materials 1 for more discussion. Given that diet $d_{i,j} = 0$ for each column j associated with autotrophs or detritus, consumption $\bar{c}_{i,j} = 0$ and $c_{i,j}(t) = 0$ for autotrophs and detritus as well.

Loss rates $m_s(t)$ are calculated separately for detritus and biomass variables. Specifically, loss for biomass variables (autotrophs and heterotrophs) results from consumption and unmodeled natural mortality, while loss for detritus results from consumption and a constant export rate:

$$m_s(t) = \underbrace{\frac{\sum_{j=1}^{S} c_{s,j}(t)}{\beta_s(t)}}_{\text{Predation rate}} + \begin{cases} \underbrace{p_s(1-e_s)}_{\substack{\text{Residual natural} \\ \text{mortality rate}}} & \text{if } s \text{ is autotroph or heterotroph} \\ \underbrace{v_s}_{\text{Export rate}} & \text{if } s \text{ is detritus} \end{cases} \tag{5}$$

where residual natural mortality $p_s(1 - e_s)$ accounts for predation by unmodeled taxa, senescence, and disease. As a taxon s has more predators explicitly modeled, ecotrophic efficiency $e_s \to 1$ such that residual mortality $p_s(1 - e_s) \to 0$, while a taxon with no modeled predators ($e_s = 0$) will have residual natural mortality of p_s. This one-to-one relationship between residual mortality and ecotrophic efficiency (for a given production per biomass) is necessary to achieve mass-balance, such that the proportion of consumptive vs. residual natural mortality for each taxon is determined upon how many of its predators are represented.

Similarly, v_s is detritus export (e.g., decomposition or turnover) rate, which is defined to ensure that net detritus accumulation matches net consumption plus export at equilibrium:

$$\bar{\beta}_s v_s = \underbrace{\sum_{i=1}^{S}\sum_{j=1}^{S} u_j \bar{c}_{i,j}(t) + \sum_{j=1}^{S} \bar{\beta}_j p_s (1 - e_s)}_{\text{Detritus accumulation}} - \underbrace{\sum_{j=1}^{S} \bar{c}_{s,j}(t)}_{\substack{\text{Detritus} \\ \text{consumption}}} \tag{6}$$

where u_j is the proportion of consumption that is not assimilated for predator j (with $u_j = 0.2$ by default) such that total unassimilated consumption $\sum_{i=1}^{S}\sum_{j=1}^{S} u_j c_{i,j}(t)$ then accumulates as detritus. Similarly, $\sum_{s=1}^{S} p_s(1 - e_s)$ is the total residual natural mortality, which we assume flows to detritus following Walters et al. (1997).

Gain rate $g_s(t)$ is then calculated differently for producers, consumers, and detritus:

$$g_s(t) = \begin{cases} \dfrac{p_s}{w_s} \times \dfrac{\sum_{i=1}^{S} c_{i,s}(t)}{\beta_s(t)} & \text{if } s \text{ is heterotroph} \\ \dfrac{p_s \bar{\beta}_s}{\beta_s(t)} \times \dfrac{x_{s,s} \dfrac{\beta_s(t)}{\bar{\beta}_s}}{x_{s,s} - 1 + \dfrac{\beta_s(t)}{\bar{\beta}_s}} & \text{if } s \text{ is autotroph} \\ \dfrac{\sum_{i=1}^{S}\sum_{j=1}^{S} u_j c_{i,j}(t) + \sum_{j=1}^{S} \beta_j(t) p_j (1 - e_j)}{\beta_s(t)} & \text{if } s \text{ is detritus} \end{cases} \tag{7}$$

where the gain rate for heterotrophs is calculated as total consumption across all prey divided by predator biomass, and multiplied by the ratio of production per biomass and consumption per biomass (termed growth efficiency). Alternatively, autotrophs do not consume other modeled taxa, so their density-dependence is modeled via a Michaelis-Menton (a.k.a. half-saturation) function (Walters et al. 1997 Eq. 5; Gaichas et al. 2012 Eq. 6) where $p_s \bar{\beta}_s$ is their equilibrium production and $\frac{x_{s,s} \frac{\beta_s(t)}{\bar{\beta}_s}}{x_{s,s} - 1 + \frac{\beta_s(t)}{\bar{\beta}_s}}$ has the same form as the predator functional response for heterotrophs (Eq. 4). Finally, detritus accumulates from the unassimilated consumption for all predators and

prey $\sum_{i=1}^{S}\sum_{j=1}^{S} u_j c_{i,j}(t)$, as well as unmodeled mortality rate $\sum_{j=1}^{S}\beta_j(t)p_j(1-e_j)$ for each taxon as prey (Walters et al. 1997).

Finally, EcoState estimates an instantaneous fishing mortality rate for any variable with catch data in a given year. To do so, EcoState tracks the harvest η_s for each variable s, and treats vector $(\boldsymbol{\beta}, \boldsymbol{\eta})$ of length $2S$ as the augmented set of state variables. Harvest is itself calculated from fishing mortality rates $\boldsymbol{\phi}(t)$ composed of $\phi_k(t)$ for each fishery k, where each fishery has species selectivity $r_{s,k}$ such that the fishing mortality rate for each species is $\mathbf{f}(t) = \mathbf{R}\boldsymbol{\phi}(t)$. We also include an additional process-error term $\boldsymbol{\epsilon}(t) \odot \boldsymbol{\beta}(t)$, where $\epsilon_s(t)$ represents unmodeled variation in population growth rates for taxon s.

$$\frac{d}{dt}\boldsymbol{\beta}(t) = \left(\underbrace{\mathbf{g}(t)}_{\substack{\text{Growth}\\ \text{rate}}} - \underbrace{\mathbf{m}(t)}_{\substack{\text{Natural}\\ \text{mortality}\\ \text{rate}}} - \underbrace{\mathbf{f}(t)}_{\substack{\text{Fishing}\\ \text{mortality}\\ \text{rate}}} + \underbrace{\boldsymbol{\epsilon}(t)}_{\substack{\text{Process error}\\ \text{in biomass rate}}} \right) \odot \boldsymbol{\beta}_t \tag{8}$$

$$\frac{d}{dt}\boldsymbol{\eta}(t) = \mathbf{f}(t) \odot \boldsymbol{\beta}(t)$$

Including process errors $\epsilon_{s,t}$ in the differential equation for mass (Eq. 8) implies that mass-balance is maintained on average over time, but not exactly in any single year. We interpret any short-term departure from mass-balance as representing processes that are not well approximated in the model, i.e., annual variation in ecotrophic efficiency, detrital export, growth efficiency, residual natural mortality, or resulting from unmodeled environmental conditions.

Model fitting

To fit this model, EcoState defines a set of coefficients $\boldsymbol{\theta} = (\mathbf{p}, \mathbf{w}, \mathbf{D}, \bar{\boldsymbol{\beta}}, \boldsymbol{\phi}(t), \boldsymbol{\delta}, \boldsymbol{\epsilon}(t), \mathbf{q}, \boldsymbol{\sigma}^2, \boldsymbol{\tau}^2, \boldsymbol{\nu}^2)$. These are then used to project biomass $\boldsymbol{\beta}(t)$ through time and model predictions are compared with available data to calculate a joint likelihood. We

then treat process errors $\boldsymbol{\epsilon}(t)$ as random effects, and integrate across their values using the Laplace approximation to calculate the marginal likelihood, which is feasible at high precision because we are using automatic differentiation (Skaug and Fournier 2006). We optimize the log-marginal likelihood to identify the maximum-likelihood estimate for selected parameters, and compute Empirical Bayes predictions of random effects by optimizing the joint likelihood with respect to random effects using the MLE for fixed effects. Finally, we use a generalization of the delta method to compute standard errors and predictive errors for fixed and random effects (Kass and Steffey 1989). EcoState is implemented in the R statistical environment (R Core Team 2023) using RTMB (Kristensen 2024a). RTMB provides a simplified interface to the Template Model Builder library (Kristensen et al. 2016), which uses automatic differentiation (AD) for efficient calculation of model derivatives, as well as the derivative of the Laplace approximation. We check model convergence by confirming that the gradient of the log-marginal likelihood with respect to each fixed effect is less than 0.001, and the matrix of 2nd derivatives of the negative log-marginal likelihood (the outer Hessian matrix) is positive definite;

In the following, we assume that the diet matrix **D** is known, and explore either fixing **p** and **w** or estimating **p** and **w** using informative Bayesian priors. We encourage future research to adapt Bayesian diagnostics for ecosystem-modelling contexts (Monnahan 2024), but do not explore it in detail here. Similarly, the user can control what combination of other parameters are estimated or fixed at known values. In particular, the user must specify (or estimate) a value for either ecotrophic efficiency e_s or equilibrium biomass $\bar{\beta}_s$ (but not both) for each taxon, and EcoState then solves for the unspecified value (e.g., e_s if $\bar{\beta}_s$ is treated as a parameter) for each taxon (see Supplementary Materials 2). This specified value can be fixed *a priori* (e.g., fixing ecotrophic efficiency $e_s = 1$ for a taxon s for which all predators are modeled) or estimated as a

fixed effect (e.g., estimating equilibrium biomass $\bar{\beta}_s$ for a taxon that has an absolute index of biomass to inform population scale, or fishery depletion is informative about population scale). We therefore estimate equilibrium biomass and/or ecotrophic efficiency for some set of taxa, while jointly projecting biomass $\beta_s(t)$ in discretized times $t \in \{1,2,\dots,T\}$.

We specifically assume that the biomass β_s for each variable s starts at some initial condition, $\beta_s(t_1) = \bar{\beta}_s \delta_s$, where δ_s is the ratio of initial to equilibrium mass for taxon s, where $\log(\delta_s) = 0$ by default. At the beginning of each time-interval, we similarly specify that annual harvest $\boldsymbol{\eta}(t) = \mathbf{0}$ for all taxon. We then integrate the differential equation over the interval $(t, t+1)$ using specified values of $\mathbf{p}, \mathbf{w}, \mathbf{e}, \mathbf{D}, \overline{\boldsymbol{\beta}}, \boldsymbol{\phi}(t)$ and $\boldsymbol{\epsilon}(t)$, and record the integrated value $\boldsymbol{\eta}(t+1)$ at the end of each interval as the predicted catch occurring for each taxon in that interval from t to $t+1$. In the following, we specifically use a third-order Adams-Bashford-Moulton method, but also provide an alternative fourth-order Runge-Kutta method where both are adapted from the *pracma* package in R (Borchers 2023). We initially explored alternative ordinary differential equation (ODE) solvers that are provided by the *deSolve* package in R (Soetaert et al. 2010) using package *RTMBode* (Kristensen 2024b), but found that this approach was not sufficiently flexible to deal with the Laplace approximation given the specified structure of EcoState. We continue this integration for all $t \in \{1,2,\dots,T\}$, while recording biomass $\boldsymbol{\beta}(t)$ and harvest $\boldsymbol{\eta}(t)$ at the end of each year. We confirmed that results are unchanged when increasing the number of subintervals evaluated when applying the ODE solver for Eq. 8.

We then calculate the joint likelihood by specifying that biomass measurements follow a lognormal distribution:

$$\log(b_s(t)) \sim \text{Normal}(\log(q_s \beta_s(t)), \sigma_s^2) \quad (9)$$

where q_s is the catchability coefficient representing the proportion of biomass that is available to a monitoring program for taxon s, σ_s^2 is a user-specified variance for the any biomass measurements, and where $b_{s,t} = \text{NA}$ ignores this component from the likelihood. Similarly, we specify a lognormal distribution for catches:

$$\log(h_s(t)) \sim \text{Normal}(\log(\eta_s(t)), \nu_s^2) \quad (10)$$

where ν_s^2 is a user-specified variance for the any catch data, and where $h_s(t) = \text{NA}$ ignores this component from the likelihood. Finally, we specify a distribution for process errors:

$$\epsilon_s(t) \sim \text{Normal}(0, \tau_s^2) \quad (11)$$

where τ_s^2 and $\boldsymbol{\epsilon}_s$ can be fixed at zero *a priori* to "turn off" process errors for any taxa s, or τ_s^2 can be estimated as a fixed effect and $\boldsymbol{\epsilon}_s$ as a random effect.

Case study: productivity and mortality for Alaska pollock in the eastern Bering Sea

To illustrate the potential benefits of hierarchical ecosystem models using EcoState, we fit it to survey data and catches for 11 variables in the eastern Bering Sea from 1982-2021 (Table S2). This example includes major predators, prey, and competitors for Alaska pollock, including three fishes (pollock; Pacific cod, *Gadus macrocephalus*, hereafter referred to as cod; and arrowtooth flounder *Atheresthes stomias*), one autotroph (pelagic producers), one detritus variable, five intermediate consumers (copepods, krill, demersal invertebrates, benthic microbes, and other pelagic zooplankton), and one predator (northern fur seal, *Callorhinus ursinus*). We use productivity and diet parameters ($\mathbf{p}, \mathbf{w}, \mathbf{D}$, see Table S3) from previous Rpath and EwE analysis (Aydin et al. 2007; Whitehouse et al. 2021), which are aggregated using biomass-weighted averages from those models. However, we use updated consumption w_s for northern fur seals to better account for energy needs while in the eastern Bering Sea. We do not use any information about ecosystem scale (ecotrophic efficiency e_s or equilibrium biomass $\overline{\beta_s}$) from a previous

379 mass-balance model, to avoid "double-dipping" on data that might have informed previous
380 models and which we also use during model fitting. We fit the model using 20 sub-intervals for
381 the Adams-Bashforth solver per year, but confirm that results are (essentially) unchanged when
382 increasing this to 30 sub-intervals per year.

383 This example estimates annual fishing mortality using catch data for the three fishes
384 (pollock, cod, and arrowtooth founder). We assume that catches arise from three separate
385 fisheries (i.e., the fishery selection matrix **R** is an identity matrix), and specify measurement
386 error $\nu_s = 0.1$. We also fit to biomass time-series calculated using a design-based estimator
387 applied to survey data from an annual bottom-trawl survey in the eastern Bering Sea (Lauth and
388 Conner 2016), and a biomass-time series for northern fur seal (from McHuron et al. 2020), and
389 see Supplementary Materials 3 for details. Cod and arrowtooth are bottom-associated species,
390 and we therefore assume that the biomass time-series in the eastern Bering Sea is an absolute
391 index of biomass (i.e., catchability coefficient $q_s = 1$). Similarly, the northern fur seal biomass
392 index is generated from population models estimating numbers at age for St. Paul and St. George
393 Islands (we only use values from years with direct surveys occurring at those sites), and we also
394 assume that it is an absolute index of biomass. Given this assumption, we then estimate
395 equilibrium biomass $\bar{\beta}_s$ and initial abundance relative to equilibrium δ_s for cod, arrowtooth, and
396 northern fur seal as fixed effects. By contrast, pollock has both demersal and pelagic
397 components (Monnahan et al. 2021), so we treat the bottom-trawl survey as a relative abundance
398 index and therefore estimate catchability q_s (which we expect will be < 1) and initial abundance
399 relative to equilibrium δ_s. Similarly, we fit to a relative abundance index (i.e., estimating
400 catchability coefficient q_s) for biomass indices for copepods and other pelagic zooplankton

401 (from a fall surface trawl survey), krill (from a summer acoustics survey), and pelagic primary
402 producers (from satellite chlorophyll-*a* concentrations averaged from May to October).
403 For all eight variables without an absolute biomass index, we estimate population scale
404 by specifying that ecotrophic efficiency $e_s = 1$. However, future applications could instead use
405 Bayesian priors on ecotrophic efficiency and/or equilibrium biomass to relax the assumption that
406 $e_s = 1$ for those eight variables. Specifying $e_s = 1$ results in all mortality being due to
407 consumption for these functional groups (i.e., residual mortality $p_s(1 - e_s) = 0$), such that
408 predator and prey are tightly coupled. We specify measurement error $\sigma_s = 0.1$ for all abundance
409 indices. We also specify vulnerability $x_{i,j} = 2$ (the default from Rpath and EwE) for all
410 heterotrophs, and $x_{i,j} = 91$ (the upper bound from Rpath) for the autotroph. Finally, we estimate
411 annual process errors for five taxa (pollock, cod, arrowtooth, copepods, and northern fur seal) as
412 random effects, and estimate the standard deviation of process-error variation τ_s for each of these
413 taxa as fixed effects.
414 We specifically compare estimates from four contrasting specifications of EcoState:
415 1. *Full*: Estimating process errors and fishing mortality, to estimate annual consumption and
416 productivity resulting from estimated biomass for predators and prey;
417 2. *Priors*: Estimating the same model as *Full*, but also estimating productivity per biomass p_s
418 and consumption per biomass w_p for each of pollock, cod, arrowtooth, copepods, northern
419 fur seal, and euphausiids, while specifying a lognormal likelihood penalty with a log-
420 standard deviation of 0.1;
421 3. *No process errors*: Turning off process errors, to estimate the consumption and productivity
422 that would be expected without estimating annual variation in ecological dynamics;

4. *No catches or process errors*: Turning off process errors and ignoring fishing mortality (i.e., specifying $h_s(t) = 0$ for all taxa), to estimate the equilibrium conditions that are otherwise expected.

Finally, we also extract a comparable measure of combined (male and female) biomass from stock-assessment models where available, e.g., total biomass for Pacific cod using model 23.1.0.d (S. Barbeaux et al., 2024 Table 2.26), age 3+ biomass for Alaska pollock (Ianelli et al., 2023 Table 26), and age-1+ biomass for arrowtooth flounder (Shotwell et al., 2023 Table 6.13).

For each model, we record annual growth rate $g_s(t)$ and mortality rate $m_s(t)$. We use this to illustrate how variation in predators and prey has resulted in time-varying production. We also decompose growth-rate and mortality-rate per biomass into the contributions from individual predators and prey species (additive components of Eq. 7 and 5, respectively), so that we can attribute changes in production to individual prey and predators. Fitting the full model with uninformative starting values required approximately 2 hours on a standard laptop using R version 4.3.0.

Simulation experiment: estimating productivity and mortality

To explore the statistical performance of EcoState, we also conduct a "self-test" simulation experiment. The experiment involves simulating ecosystem dynamics, simulating abundance indices and catch data, refitting the model to these data with or without estimating process errors, and comparing estimates with known (true) values of ecosystem variables for each of 50 simulation replicates. It explores whether a hierarchical ecosystem model (i.e., estimating process errors) improves estimates of growth rates $g(t)$ and mortality rates $m(t)$ relative to the common practice of ignoring process errors. We also estimate equilibrium biomass $\bar{\beta}_s$ and the

445 variance of process errors for each taxon, such that the experiment confirms whether these
446 parameters are estimable in an idealized setting.

447 We specifically simulate dynamics for a fictive ecosystem involving six taxa (see Table
448 S4): one autotroph (representing pelagic primary production), one detritus (the base of the
449 benthic foodweb), two consumers (one pelagic and one benthic), and two predators (one pelagic
450 and one benthic) from 1980-2020. We also specify that benthic consumers and predators have
451 slower life-history (lower p_s and higher w_s) than their pelagic counterparts. We specify that
452 ecotrophic efficiency $e_s = 0.9$ (i.e., 90% of biomass transfer is captured) for the producers and
453 consumers, and that predators have equilibrium biomass $\overline{\beta_s} = 1$, and then solve for equilibrium
454 biomass for the other species (see Fig. 1). Finally, we specify a vulnerability $x_{ij} = 2$
455 (representing a Hollings Type-2 predator functional response) for consumers and predators, and
456 a vulnerability $x_{ij} = 91$ (representing a close-to-constant production-per-biomass) for producers.

457 We then simulate an increase in fishing mortality rate for the two predators over the 40
458 years of simulated dynamics (see Fig. S1), and specify that process errors have a standard
459 deviation $\tau_s = 0.1$ for primary producers and predators, and $\tau_s = 0.02$ for consumers (which are
460 also affected by process errors in both predators and producers). We simulate abundance indices
461 and measurements of catch for each species. We then refit the model using 10 sub-intervals of
462 the Adams-Bashforth-Moulton ODE solver. For the "full model" we estimate the difference
463 between equilibrium and initial biomass δ_s and the magnitude of process errors τ_s for each
464 taxon, as well as a single vulnerability $x_{shared} = x_{ij}$ for all consumers and predators (i.e., 13
465 fixed effects). We compare this with a "null model" that estimates only δ_s and x_{shared} (i.e., 7
466 fixed effects), and ignores process errors. Finally, we compare error in estimates of model
467 parameters, as well as annual growth rate per biomass $g_s(t)$ (Eq. 8), mortality rate per biomass

$m_s(t)$ (Eq. 6), and biomass $\beta_s(t)$ between the full and null models. We then repeat the experiment when estimating production per biomass p_s for all six taxa and consumption per biomass w_s for the four heterotrophs (10 extra parameters), while specifying a lognormal likelihood penalty with a log-standard deviation of 0.1. Each replicate of the simulation model required approximately 10 min on a standard laptop using R version 4.3.0.

Results

For the eastern Bering Sea case study, the full version of the EcoState model (i.e., including 11 variables and fitting to catches using process errors) includes both benthic and pelagic sources of production (Fig. 1 and Table S3), and has variables that range from trophic level 1 (producer and detritus) to 4.3 (northern fur seal). Estimated trends and interannual variation are consistent with biomass surveys (except for copepods, Fig. 2), and are also consistent with recent stock assessments when available (i.e., for pollock, cod, and arrowtooth flounder; Fig. 3). Major consumers (pollock and cod) show biomass cycles, i.e., elevated biomass from 2000-2005 and decreased biomass from 2005-2010, followed by elevated biomass from 2012-17 and subsequently lower biomass. By contrast, arrowtooth flounder, northern fur seal, and zooplankton are dominated by decadal trends, i.e., arrowtooth showed a large increase in biomass from 1982-1990, northern fur seal showed a progressive decrease in biomass from 1995 onward, and both krill and primary producers both show a pronounced decline from 2008 onward. As expected, pollock biomass is higher than the bottom-trawl survey index due to an estimated catchability coefficient less than one, i.e., $\log(q_s) = -0.41$, and closely fits specified catch data (Fig. S3).

The increasing biomass trend for arrowtooth and decreasing trend for northern fur seal are largely explained by the estimated difference between initial and equilibrium biomass

491 ($\log(\delta_s) = -2.42$ and 0.27, respectively; see Table S5). As a result, the trends for these taxa are
492 also captured by models that ignore process errors, or the null model without process errors or
493 catches (Fig. 3). However, the model without process error (blue line in Fig. 3) only captures a
494 dampened version of the biomass cycles for Pacific cod, and fails to capture the biomass cycles
495 for pollock or trends for the other species. Similarly, the model without process errors and
496 catches estimates lower biomass overall for zooplankton (krill, copepods, and other), pollock,
497 and benthic variables. This difference in scale in the model without catches arises because we
498 specify ecotrophic efficiency $e_s = 1$ for intermediate consumers (to avoid using auxiliary
499 information to define their population scale). Without fishery harvest, the model can decrease
500 copepod biomass from 4 to 2 million tons while still maintaining the biomass of species with
501 indices of absolute abundance (cod, arrowtooth, and northern fur seals). Similarly, the model
502 using Bayesian priors (instead of fixed values) for production and consumption per biomass ($\mathbf{p}$
503 and $\mathbf{w}$) estimates somewhat different biomass for pollock and planktonic taxa (krills, copepods,
504 etc) but otherwise similar patterns in biomass (Fig. 3).

505 The state-space model attributes biomass patterns to annual variation in growth $g(t)$,
506 natural mortality $m(t)$, fishing mortality $f(t)$ for the three exploited fishes (Fig. 4), and process
507 errors (Fig. S3). The model captures substantial variation in growth rate $g(t)$ for these species
508 because it includes the primary forage for each modeled functional group. It captures less
509 variation mortality rates $m(t)$ because it has fewer top-predators, such that cod and arrowtooth
510 have lower ecotrophic efficiency e_i, and therefore attributes mortality $m(t)$ primarily to the
511 constant mortality term $u_s = p_s(1 - e_s)$ (e.g., the pink bars for cod mortality in Fig. 5). Growth
512 exceeds natural and fishing mortality rates for arrowtooth during the initial years (1982-1995),
513 which drives an increase in biomass, and this difference subsequently declines towards zero as

514 population biomass stabilizes. Similarly, northern fur seals have lower growth than natural
515 mortality, in particular from 1995-2000 and again 2005-2015, which drives a decline in biomass
516 over time. However, biomass patterns cannot be entirely explained by changes in consumption
517 driving growth and natural mortality. Cod and pollock have lower-than-average biomass from
518 2005-2010, and density dependence causes estimated growth to exceed natural mortality rates
519 (Fig. 4); however, this density-dependent increase in productivity is offset by negative process
520 errors $\epsilon_s(t)$ (Fig. S3), which allows the model to estimate that lower-than-average biomass
521 persists over these years. Similarly, decadal trends for northern fur seal are driven by a sequence
522 of positive process errors until 2000 followed by negative process errors.
523 The model can be used to further decompose growth and mortality rates into the
524 contribution of individual prey and predator species, respectively (Fig. 5). This exercise shows
525 that elevated growth rates for pollock during positive cycles (top-left panel of Fig. 5) are
526 associated with an increased proportion of krill consumption, while the contribution of copepods
527 to pollock growth rate has been relatively consistent over time. Predation on pollock shows a
528 small but noticeable increase when arrowtooth biomass increased from 1982-1990 (bottom-left
529 panel of Fig. 5). However, fluctuations in pollock mortality are largely due to changes in
530 cannibalism from pollock and predation from cod, during their population cycles. By contrast,
531 growth rate for cod largely follows the cycles for pollock as their major prey (red in top-right
532 panel of Fig. 5). We do not explicitly model many predators for cod, and hence their natural
533 mortality is largely attributed to the residual mortality that is constant over time. Finally, krill
534 has higher growth and mortality rates than either pollock or cod due to their faster life-history,
535 and this means that small relative differences (e.g., changing growth $g_s(t)$ from 6 to 5.8) can still
536 result in large absolute differences in population dynamics. However, the decline in chlorophyll

biomass in 2010 (Fig. 2) is immediately apparent in decreased consumption and growth-rate for krill (Fig. 5), which is synchronous with the decrease in krill biomass around that time.

Finally, our self-test simulation experiment confirms the state-space model can accurately estimate annual growth $g(t)$ and mortality $m(t)$ components (red line in Fig. 6), and generally was more precise than a model that does not estimate process errors (blue line in Fig. 6). This difference results from the ability of the state-space model to more-accurately estimate annual variation in biomass for predators and prey, and therefore also improves the estimates of consumption $c_{s_2,s_1}(t)$ and resulting estimates of predator growth and prey mortality rates. Both the full and null models can accurately estimate the vulnerability and equilibrium biomass parameters (see Fig. S4). We also replicate the simulation experiment while estimating productivity per biomass **p** and consumption per biomass **w** using Bayesian priors. The full model continues to outperform the model without process errors, although both models have substantially higher errors for producers and detritus (Fig. S5).

Discussion

We have argued that hierarchical (a.k.a. state-space) modelling will have broad benefits across the full range of ecosystem models. These benefits include (1) better representation of system trends and cycles; (2) propagating errors through species interactions; (3) reproducibility during model fitting; and (4) attributing process errors to different mechanisms. We have then demonstrated these benefits using the first (to our knowledge) state-space extension of the most widely used mass-balance model[1] in fisheries (Colléter et al. 2015). This extension jointly estimates mass-balance parameters and process errors via fit to time-series data. Including

[1] Ecopath with Ecosim has 487 models compiled online via EcoBase (https://ecobase.ecopath.org/) as accessed June 11, 2024.

process errors allows us to capture decadal trends and interannual cycles in biomass (which are otherwise mis-specified in a model that does not have process errors, Fig. S3), and to more accurately capture the variable growth and mortality rates that result from changes in consumption. Estimating parameters via maximum likelihood also allows us to propagate variance in both fixed effects (e.g., equilibrium biomass) and process errors when predicting biomass in unsampled years. This predictive variance includes the contribution of both fixed effects and process errors, such that biomass has higher predictive uncertainty when distant from available data and/or for taxa with rapid life-histories. We distribute our code as an R package *EcoState*, initially available on GitHub (https://github.com/James-Thorson-NOAA/EcoState) with full function documentation and user vignettes (and intended for distribution via CRAN upon full release) to facilitate ongoing applications and testing.

Although we extended Ecopath with Ecosim here, we suspect that a wide range of ecosystem analyses could be re-cast as hierarchical models using modern statistical-computing tools (e.g., RTMB as used here). This demonstration joins a growing list of hierarchical ecosystem models where, e.g., the length-structured model Mizer has options to estimate demographic rates (Spence et al. 2016) and process errors (Spence et al. 2021) via fit to time-series data. Similarly, multispecies statistical catch-at-age models often estimate recruitment deviations while accounting for predator-dependent mortality (i.e., top-down control) but not consumption-dependent growth (i.e., bottom-up control), and are sometimes called "Models of Intermediate Complexity for Ecosystems" (Plagányi et al. 2014). Despite these examples, hierarchical modelling has not previously been adopted for widely used ecosystem models including Ecopath with Ecosim, Atlantis (Fulton et al. 2011), or Osmose (Shin and Cury 1999). In these cases, modelers typically explore uncertainty by sampling parameters from a specified

distribution and summarizing the resulting distribution for model outputs, e.g., in Osmose (Luján et al. 2024), the Rpath implementation of Ecopath with Ecosim (Whitehouse and Aydin 2020), or Atlantis (Fulton et al. 2011). Additionally, software for these models sometimes can estimate a subset of parameters, e.g., fitting vulnerability ($x_{i,j}$) parameters in Ecosim via fit to time-series without otherwise estimating parameters that arise in the Ecopath mass-balance itself (Scott et al. 2016; Bentley et al. 2024), or the "anomaly search" function that explains model residuals using specified covariates (Shannon et al. 2008). By contrast, automatic differentiation (e.g., RTMB) allows efficient calculation of the gradient of the log-likelihood function with respect to parameters, which allows us to estimate hundreds of coefficients (random and fixed effects) with little additional code beyond implementing the model dynamics themselves. We therefore encourage research exploring the use of RTMB for other classes of ecosystem models, where penalized likelihood (i.e., fixing process-error variance *a priori*) would be easier (and therefore appropriate for more complex models) than the maximum-likelihood estimation used here.

We believe that hierarchical modelling will help to mitigate capacity constraints that limit the use of ecosystem and multispecies models for short-term fisheries management. Ecosystem modelers typically have just a few years to develop a "research" model and then show its usefulness for management. Optimizing parameters based on statistical fit to time-series allows modelers in the related field of stock assessment to rapidly explore hundreds of different scenarios (from different combinations of estimated parameters and assumed model structure) when incorporating new data or addressing reviewer or stakeholder input. In particular, estimating process errors (e.g., recruitment deviations in age-structured assessments or process errors here) tends to allow models to have reasonable behavior (i.e., continue to track major trends) when updated with new data, as required for an operational model that will be

604 subsequently updated. Including fewer species (as we do here) can also address capacity
605 limitations by (1) reducing model implementation time as an analyst could focus on developing a
606 smaller set of data inputs, (2) simplifying the peer review process, and (3) reducing model run
607 time thus allowing more time for running different management scenarios. However, using a
608 smaller set of taxa also has drawbacks, i.e., it narrows the range of alternate pathways for trophic
609 interactions, and therefore may result in stronger predator-prey interactions than those estimated
610 when including more taxa. Future analysis could also explore whether the variance of process
611 errors is reduced when adding functional groups.

612 This state-space mass-balance model can also be interpreted as a mechanistic model to
613 incorporate time-varying productivity into biomass-dynamic (a.k.a., surplus production) models.
614 Biomass-dynamic models are one of the oldest models in ecology (Pearl and Reed 1920) and
615 fisheries (Russell 1931), and state-space extensions are still widely used to identify stock status
616 for many fisheries worldwide (Pedersen and Berg 2017; Winker et al. 2020). These models
617 typically estimate population scale (equilibrium biomass and a catchability coefficient) by
618 treating the fishery as a depletion experiment (Magnusson and Hilborn 2007). We encourage
619 future research to compare EcoState against state-space biomass-dynamics models. In particular,
620 EcoState would provide a parsimonious approach to predict nonstationary parameters resulting
621 from changing predator or prey biomass (Aydin 2004), while allowing estimates of the
622 catchability coefficient in some cases. We hypothesize that trophic interactions could result in
623 population-cycles that are otherwise missing from single-species biomass-dynamic models
624 (Walters and Kitchell 2001), and could also change the shape of the production function (and
625 resulting biological reference points).

626 Our case-study illustrates several of our claimed advantages of hierarchical ecosystem
627 modelling. Specifically, the ecosystem includes both cyclic and long-term biomass trends that
628 are not well captured by a mass-balance model without process errors (also noted by Aydin and
629 Mueter 2007). In particular, primary producers have declined by nearly 30%, and this is
630 synchronous with a declining trend in krill biomass. Previous studies have debated the relative
631 importance of top-down and bottom-up control for krill biomass (Ressler et al. 2012, 2014), and
632 our study identifies declining chlorophyll-a concentrations (and its impact on growth) as a
633 potential mechanism (see Fig. 4 bottom-left panel). The model then attributes a small decline in
634 productivity for pollock to this depressed krill biomass. These types of multi-level bottom-up
635 impacts are not represented by statistical multispecies models, and emphasizes the importance of
636 improved monitoring for krill in understanding climate-impacts on ecosystem productivity.
637 However, we note that bottom-up forcing is also favored by model assumptions, i.e., assuming
638 ecotrophic efficiency $e_i = 1$ for prey groups (thus eliminating non-predation natural mortality)
639 and assuming that vulnerability $x_{i,j} = 2$. In particular, future studies should seek to identify
640 whether declining primary producers is associated with an increase in consumption w_s and/or
641 production p_s per biomass, which could offset the food-web impacts of declining primary
642 producers (Nielsen et al. 2023).
643 Our case-study also illustrates how hierarchical ecosystem modelling allows us to
644 compare across alternative model structures using a small set of modeled taxa. Recent Rpath
645 models for the eastern Bering Sea have included nearly 100 taxa (Aydin et al. 2007; Whitehouse
646 et al. 2021), and the resulting model is typically used to evaluate strategic (long-term) tradeoffs
647 among management strategies. By contrast, our EcoState model includes only 10 functional
648 groups and one detrital pool; this small size is relatively rare for mass-balance models (although

see Chagaris et al. 2020), although pooling taxa still results in nearly 80% of biomass from the full Rpath model being included (see Supplementary Materials S3). Including fewer taxa allows us to calculate a high-accuracy solution to the differential equation for biomass while still integrating across random effects, as required when estimating the variance of process errors. It also allows us to provide a statistically rigorous prediction of ecosystem variables (and associated uncertainty) beyond the range of abundance indices. These predictions could then be used for seasonal-to-decadal forecasting, identifying annual status relative to ecosystem targets, or other tactical (short-term) management decisions (Plagányi 2007). Real-world application could compare model performance using an ensemble of simple-to-complex models using EcoState, and could evaluate performance both statistically or by identifying a reduction in process error variance (see 4th benefit of hierarchical models in the Introduction).

Finally, we recommend that hierarchical models (whether in stock assessment or ecosystem models) are used to attribute process errors to additional oceanographic, ecological, physical drivers. We have specified that process errors are independent and identically distributed, but recent research has demonstrated how to specify a dynamic structural equation model (DSEM) representing lagged and simultaneous causal effects among process errors (Thorson et al. 2024). We therefore envision that future studies could treat annual covariates (e.g., ocean temperature or predator-prey overlap) as additional model variables that are treated as measured without error, and then estimate how these covariates then affect process errors. This is somewhat akin to the "forcing functions" that are estimated using covariates in Ecopath-with-Ecosim, although DSEM would allow missing covariate values to be imputed based on temporal and multivariate correlations, similar to recent practices in stock assessment (du Pontavice et al. 2022). For example, previous research suggests that the summer "cold pool"

affects predator-prey overlap (Thorson et al. 2021), and this in turn affects predator consumption and diet composition (Goodman et al. 2022). These types of causal chains can be represented using DSEM and allow detailed specification of how covariates affect modeled processes. Once the magnitude and trend for process errors has been estimated using a hierarchical model, it then opens up a huge scope for additional research to attribute these patterns to hypothesized ecosystem drivers.

Acknowledgements

We thank Sean Lucey for previous research developing Rpath, and Arnaud Grüss, Greig Oldford, and two anonymous reviewers for helpful comments on a previous draft. Data were collected by many programs at the Alaska Fisheries Science Center, and we thank the midwater acoustics and conservation engineering (MACE) program for developing the krill index, the groundfish assessment program (GAP) for collecting the bottom-trawl survey data, the Recruitment Process Program (RPP) for collecting the copepod and other pelagic zooplankton samples, the Alaska Ecosystem Program (AEP) for collecting the northern fur seal data, and the Fisheries Monitoring and Analysis (FMA) Division for collecting fishery data that is used to estimate fishery harvest. We also thank the assessment authors for pollock (J. Ianelli), cod (S. Barbeaux), and arrowtooth (I. Spies) for prior research regarding the fished species. This publication is EcoFOCI contribution number EcoFOCI-1062. It is partially funded by the Cooperative Institute for Climate, Ocean, & Ecosystem Studies (CICOES) under NOAA Cooperative Agreement NA20OAR4320271, Contribution No. 2024-1391.

Data Availability Statement

All data and code are included in R-package *EcoState* release 0.1.0 (https://github.com/James-Thorson-NOAA/EcoState), which is available as a public GitHub repository during review, and

intended for submission to CRAN upon acceptance. *EcoState* release 0.1.0 includes three vignettes that can be viewed online (https://james-thorson-noaa.github.io/EcoState) or replicated locally: (1) "simulation" shows how to fit the simulated 6-species ecosystem using EcoState, and contrasts it with package Rpath; (2) "surplus production" shows how to fit single-species data simulated using a Fox production function as a state-space biomass-dynamics model using EcoState, and contrasts fit with JABBA (Winker et al. 2024) and SPiCT (Pedersen and Berg 2017); (3) "eastern Bering Sea" shows how to fit the eastern Bering Sea case study involving 10 functional groups and 1 detritus pool.

Works cited

Aydin, K., Gaichas, S., Ortiz, I., Kinzey, D., and Friday, N. 2007. A comparison of the Bering Sea, Gulf of Alaska, and Aleutian Islands large marine ecosystems through food web modeling. U.S. Dep. Commer. Available from https://repository.library.noaa.gov/view/noaa/22894/noaa_22894_DS1.pdf.

Aydin, K., and Mueter, F. 2007. The Bering Sea—A dynamic food web perspective. Deep Sea Res. Part II Top. Stud. Oceanogr. **54**(23): 2501–2525. doi:10.1016/j.dsr2.2007.08.022.

Aydin, K.Y. 2004. Age structure or functional response? Reconciling the energetics of surplus production between single-species models and ecosim. Afr. J. Mar. Sci. **26**: 289–301.

Begley, J., and Howell, D. 2004. An overview of Gadget, the globally applicable area-disaggregated general ecosystem toolbox. ICES. Available from https://imr.brage.unit.no/imr-xmlui/bitstream/handle/11250/100625/FF1304.pdf?sequence=1 [accessed 11 June 2024].

Bentley, J.W., Chagaris, D., Coll, M., Heymans, J.J., Serpetti, N., Walters, C.J., and Christensen, V. 2024. Calibrating ecosystem models to support ecosystem-based management of marine systems. ICES J. Mar. Sci. **81**(2): 260–275. doi:10.1093/icesjms/fsad213.

Borchers, H.W. 2023. pracma: Practical Numerical Math Functions. Available from https://CRAN.R-project.org/package=pracma.

Chagaris, D., Drew, K., Schueller, A., Cieri, M., Brito, J., and Buchheister, A. 2020. Ecological Reference Points for Atlantic Menhaden Established Using an Ecosystem Model of Intermediate Complexity. Front. Mar. Sci. **7**. Frontiers. doi:10.3389/fmars.2020.606417.

Christensen, V., and Walters, C.J. 2004. Ecopath with Ecosim: methods, capabilities and limitations. Ecol. Model. **172**(2): 109–139. doi:10.1016/j.ecolmodel.2003.09.003.

Colléter, M., Valls, A., Guitton, J., Gascuel, D., Pauly, D., and Christensen, V. 2015. Global overview of the applications of the Ecopath with Ecosim modeling approach using the EcoBase models repository. Ecol. Model. **302**: 42–53. doi:10.1016/j.ecolmodel.2015.01.025.

du Pontavice, H., Miller, T.J., Stock, B.C., Chen, Z., and Saba, V.S. 2022. Ocean model-based covariates improve a marine fish stock assessment when observations are limited. ICES J. Mar. Sci. **79**(4): 1259–1273. doi:10.1093/icesjms/fsac050.

Edwards, A.M., and Auger-Méthé, M. 2019. Some guidance on using mathematical notation in ecology. Methods Ecol. Evol. **10**(1): 92–99. doi:10.1111/2041-210X.13105.

European Commission. 2013. REGULATION (EU) No 1380/2013 OF THE EUROPEAN PARLIAMENT AND OF THE COUNCIL. EUROPEAN PARLIAMENT AND OF THE COUNCIL, Brussels.

FAO. 2003. Fisheries management. The ecosystem approach to fisheries. UN Food and Agriculture Organization, Rome.

Felsenstein, J. 1985. Phylogenies and the Comparative Method. Am. Nat. **125**(1): 1–15. doi:10.1086/284325.

Fulton, E.A., Link, J.S., Kaplan, I.C., Savina-Rolland, M., Johnson, P., Ainsworth, C., Horne, P., Gorton, R., Gamble, R.J., Smith, A.D.M., and Smith, D.C. 2011. Lessons in modelling and management of marine ecosystems: the Atlantis experience. Fish Fish. **12**(2): 171–188. doi:10.1111/j.1467-2979.2011.00412.x.

Gaichas, S.K., Odell, G., Aydin, K.Y., and Francis, R.C. 2012. Beyond the defaults: functional response parameter space and ecosystem-level fishing thresholds in dynamic food web model simulations. Can. J. Fish. Aquat. Sci. **69**(12): 2077–2094. NRC Research Press. doi:10.1139/f2012-099.

Goodman, M.C., Carroll, G., Brodie, S., Grüss, A., Thorson, J.T., Kotwicki, S., Holsman, K., Selden, R.L., Hazen, E.L., and De Leo, G.A. 2022. Shifting fish distributions impact predation intensity in a sub-Arctic ecosystem. Ecography **2022**(9): e06084. doi:10.1111/ecog.06084.

Hollowed, A.B., Bax, N., Beamish, R., Collie, J., Fogarty, M., Livingston, P., Pope, J., and Rice, J.C. 2000. Are multispecies models an improvement on single-species models for measuring fishing impacts on marine ecosystems? | ICES Journal of Marine Science | Oxford Academic. ICES J. Mar. Sci. **3**(1): 707–719.

Holt, R.D. 1997. Community modules. *In* Multitrophic interactions in terrestrial ecosystems, 36th Symposium of the British Ecological Society. Blackwell Science Oxford. pp. 333–349.

Kass, R.E., and Steffey, D. 1989. Approximate Bayesian inference in conditionally independent hierarchical models (parametric empirical bayes models). J. Am. Stat. Assoc. **84**(407): 717–726. doi:10.2307/2289653.

Kristensen, K. 2024a. RTMB: "R" Bindings for "TMB." Available from https://CRAN.R-project.org/package=RTMB.

Kristensen, K. 2024b. RTMBode: Solving ODEs with "deSolve" and "RTMB".

Kristensen, K., Nielsen, A., Berg, C.W., Skaug, H., and Bell, B.M. 2016. TMB: Automatic differentiation and Laplace approximation. J. Stat. Softw. **70**(5): 1–21. doi:10.18637/jss.v070.i05.

Lauth, R.R., and Conner, J. 2016. Results of the 2013 eastern Bering Sea continental shelf bottom trawl survey of groundfish and invertebrate resources. NOAA Technical Memorandum, Alaska Fisheries Science Center, Seattle, WA.

Lucey, S.M., Gaichas, S.K., and Aydin, K.Y. 2020. Conducting reproducible ecosystem modeling using the open source mass balance model Rpath. Ecol. Model. **427**: 109057. doi:10.1016/j.ecolmodel.2020.109057.

Luján, C., Oliveros-Ramos, R., Barrier, N., Leadley, P., and Shin, Y.-J. 2024. Key species and indicators revealed by an uncertainty analysis of the marine ecosystem model OSMOSE. Mar. Ecol. Prog. Ser. **SPF2**. doi:10.3354/meps14465.

Magnusson, A., and Hilborn, R. 2007. What makes fisheries data informative? Fish Fish. **8**(4): 337–358.

McHuron, E.A., Luxa, K., Pelland, N.A., Holsman, K., Ream, R.R., Zeppelin, T.K., and Sterling J.T. 2020. Practical Application of a Bioenergetic Model to Inform Management of a Declining Fur Seal Population and Their Commercially Important Prey. Front. Mar. Sci. doi:10.3389/fmars.2020.597973.

Monnahan, C.C. 2024. Toward good practices for Bayesian data-rich fisheries stock assessments using a modern statistical workflow. Fish. Res. **275**: 107024. doi:10.1016/j.fishres.2024.107024.

780 Monnahan, C.C., Thorson, J.T., Kotwicki, S., Lauffenburger, N., Ianelli, J.N., and Punt, A.E. 2021.
781 Incorporating vertical distribution in index standardization accounts for spatiotemporal
782 availability to acoustic and bottom trawl gear for semi-pelagic species. ICES J. Mar. Sci.
783 doi:https://doi.org/10.1093/icesjms/fsab085.
784 Nielsen, A., and Berg, C.W. 2014. Estimation of time-varying selectivity in stock assessments using state-
785 space models. Fish. Res. **158**: 96–101.
786 Nielsen, J.M., Pelland, N.A., Bell, S.W., Lomas, M.W., Eisner, L.B., Stabeno, P., Harpold, C., Stalin, S., and
787 Mordy, C.W. 2023. Seasonal Dynamics of Primary Production in the Southeastern Bering Sea
788 Assessed Using Continuous Temporal and Vertical Dissolved Oxygen and Chlorophyll-a
789 Measurements. J. Geophys. Res. Oceans **128**(5): e2022JC019076. doi:10.1029/2022JC019076.
790 NOAA. 2016. Ecosystem Based Fisheries Management Policy of the National Marine Fisheries Service,
791 Policy 01-120. National Oceanic and Atmospheric Administratio, Silver Spring, MD.
792 Pauly, D., Christensen, V., and Walters, C. 2000. Ecopath, Ecosim, and Ecospace as tools for evaluating
793 ecosystem impact of fisheries. ICES J. Mar. Sci. J. Cons. **57**(3): 697.
794 Pearl, R., and Reed, L.J. 1920. On the rate of growth of the population of the United States since 1790
795 and its mathematical representation. Proc. Natl. Acad. Sci. U. S. A. **6**(6): 275.
796 Pedersen, M.W., and Berg, C.W. 2017. A stochastic surplus production model in continuous time. Fish
797 Fish. **18**(2): 226–243. doi:10.1111/faf.12174.
798 Plagányi, É.E. 2007. Models for an ecosystem approach to fisheries. Food & Agriculture Organization,
799 Rome. Available from
800 http://books.google.com/books?hl=en&lr=&id=MJI3aZApEQkC&oi=fnd&pg=PP9&dq=models+fo
801 r+an+ecoystem+approach+to+fisheries&ots=HggvLmdgLv&sig=vCbRBUVqZlUCKnWkv8I2OVbbm
802 RY [accessed 1 July 2012].
803 Plagányi, É.E., and Butterworth, D.S. 2004. A critical look at the potential of Ecopath with Ecosim to
804 assist in practical fisheries management. Afr. J. Mar. Sci. **26**: 261–287.
805 Plagányi, Punt, A.E., Hillary, R., Morello, E.B., Thébaud, O., Hutton, T., Pillans, R.D., Thorson, J.T., Fulton,
806 E.A., Smith, A.D.M., Smith, F., Bayliss, P., Haywood, M., Lyne, V., and Rothlisberg, P.C. 2014.
807 Multispecies fisheries management and conservation: tactical applications using models of
808 intermediate complexity. Fish Fish. **15**(1): 1–22. doi:10.1111/j.1467-2979.2012.00488.x.
809 Polovina, J.J. 1984. Model of a coral reef ecosystem. Coral Reefs **3**(1): 1–11. doi:10.1007/BF00306135.
810 Punt, A.E., Dunn, A., Elvarsson, B.Þ., Hampton, J., Hoyle, S.D., Maunder, M.N., Methot, R.D., and Nielsen,
811 A. 2020. Essential features of the next-generation integrated fisheries stock assessment
812 package: A perspective. Fish. Res. **229**: 105617. doi:10.1016/j.fishres.2020.105617.
813 R Core Team. 2023. R: A Language and Environment for Statistical Computing. R Foundation for
814 Statistical Computing, Vienna, Austria. Available from https://www.R-project.org/.
815 Ressler, P.H., De Robertis, A., Warren, J.D., Smith, J.N., and Kotwicki, S. 2012. Developing an acoustic
816 survey of euphausiids to understand trophic interactions in the Bering Sea ecosystem. Deep Sea
817 Res. Part II Top. Stud. Oceanogr. **65–70**: 184–195. doi:10.1016/j.dsr2.2012.02.015.
818 Ressler, P.H., Robertis, A.D., and Kotwicki, S. 2014. The spatial distribution of euphausiids and walleye
819 pollock in the eastern Bering Sea does not imply top-down control by predation. Mar. Ecol. Prog.
820 Ser. **503**: 111–122. doi:10.3354/meps10736.
821 Russell, E.S. 1931. Some theoretical Considerations on the “Overfishing” Problem. ICES J. Mar. Sci. **6**(1):
822 3–20. doi:10.1093/icesjms/6.1.3.
823 Scott, E., Serpetti, N., Steenbeek, J., and Heymans, J.J. 2016. A Stepwise Fitting Procedure for automated
824 fitting of Ecopath with Ecosim models. SoftwareX **5**: 25–30. doi:10.1016/j.softx.2016.02.002.
825 Scott, F., Blanchard, J.L., and Andersen, K.H. 2014. mizer: an R package for multispecies, trait-based and
826 community size spectrum ecological modelling. Methods Ecol. Evol. **5**(10): 1121–1125.
827 doi:10.1111/2041-210X.12256.

828 Shannon, L.J., Neira, S., and Taylor, M. 2008. Comparing internal and external drivers in the southern
829 Benguela and the southern and northern Humboldt upwelling ecosystems. Afr. J. Mar. Sci.
830 Taylor & Francis Group. doi:10.2989/AJMS.2008.30.1.7.457.
831 Shin, Y.-J., and Cury, P. 1999. OSMOSE: a multispecies individual-based model to explore the functional
832 role of biodiversity in marine ecosystems. Ecosyst. Approaches Fish. Manag. Univ. Alsk. Sea
833 Grant Fairbanks: 593–607.
834 Skaug, H., and Fournier, D. 2006. Automatic approximation of the marginal likelihood in non-Gaussian
835 hierarchical models. Comput. Stat. Data Anal. **51**(2): 699–709.
836 Soetaert, K., Petzoldt, T., and Setzer, R.W. 2010. Solving Differential Equations in R: Package deSolve. J.
837 Stat. Softw. **33**(9): 1–25. doi:10.18637/jss.v033.i09.
838 Spence, M.A., Blackwell, P.G., and Blanchard, J.L. 2016. Parameter uncertainty of a dynamic multispecies
839 size spectrum model. Can. J. Fish. Aquat. Sci. **73**(4): 589–597. NRC Research Press.
840 doi:10.1139/cjfas-2015-0022.
841 Spence, M.A., Thorpe, R.B., Blackwell, P.G., Scott, F., Southwell, R., and Blanchard, J.L. 2021. Quantifying
842 uncertainty and dynamical changes in multi-species fishing mortality rates, catches and biomass
843 by combining state-space and size-based multi-species models. Fish Fish. **22**(4): 667–681.
844 doi:10.1111/faf.12543.
845 Stock, B.C., and Miller, T.J. 2021. The Woods Hole Assessment Model (WHAM): A general state-space
846 assessment framework that incorporates time-and age-varying processes via random effects
847 and links to environmental covariates. Fish. Res. **240**: 105967.
848 Stock, B.C., Xu, H., Miller, T.J., Thorson, J.T., and Nye, J.A. 2021. Implementing two-dimensional
849 autocorrelation in either survival or natural mortality improves a state-space assessment model
850 for Southern New England-Mid Atlantic yellowtail flounder. Fish. Res. **237**: 105873.
851 doi:10.1016/j.fishres.2021.105873.
852 Thorson, J.T., Andrews III, A.G., Essington, T.E., and Large, S.I. 2024. Dynamic structural equation models
853 synthesize ecosystem dynamics constrained by ecological mechanisms. Methods Ecol. Evol.
854 **15**(4): 744–755. doi:10.1111/2041-210X.14289.
855 Thorson, J.T., Arimitsu, M.L., Barnett, L.A.K., Cheng, W., Eisner, L.B., Haynie, A.C., Hermann, A.J.,
856 Holsman, K., Kimmel, D.G., Lomas, M.W., Richar, J., and Siddon, E.C. 2021. Forecasting
857 community reassembly using climate-linked spatio-temporal ecosystem models. Ecography
858 **44**(4): 612–625. doi:https://doi.org/10.1111/ecog.05471.
859 Thorson, J.T., and Minto, C. 2015. Mixed effects: a unifying framework for statistical modelling in
860 fisheries biology. ICES J. Mar. Sci. J. Cons. **72**(5): 1245–1256. doi:10.1093/icesjms/fsu213.
861 Thorson, J.T., Ono, K., and Munch, S.B. 2014. A Bayesian approach to identifying and compensating for
862 model misspecification in population models. Ecology **95**(2): 329–341. doi:10.1890/13-0187.1.
863 de Valpine, P. 2002. Review of methods for fitting time-series models with process and observation
864 error and likelihood calculations for nonlinear, non-Gaussian state-space models. Bull. Mar. Sci.
865 **70**(2): 455–471.
866 Walters, C., Christensen, V., and Pauly, D. 1997. Structuring dynamic models of exploited ecosystems
867 from trophic mass-balance assessments. Rev. Fish Biol. Fish. **7**(2): 139–172.
868 doi:10.1023/A:1018479526149.
869 Walters, C., and Kitchell, J.F. 2001. Cultivation/depensation effects on juvenile survival and recruitment:
870 implications for the theory of fishing. Can. J. Fish. Aquat. Sci. **58**(1): 39–50.
871 Whitehouse, G.A., and Aydin, K.Y. 2020. Assessing the sensitivity of three Alaska marine food webs to
872 perturbations: an example of Ecosim simulations using Rpath. Ecol. Model. **429**: 109074.
873 Elsevier.
874 Whitehouse, G.A., Aydin, K.Y., Hollowed, A.B., Holsman, K.K., Cheng, W., Faig, A., Haynie, A.C., Hermann,
875 A.J., Kearney, K.A., Punt, A.E., and Essington, T.E. 2021. Bottom–Up Impacts of Forecasted

Climate Change on the Eastern Bering Sea Food Web. Front. Mar. Sci. **8**. Frontiers. doi:10.3389/fmars.2021.624301.

Winker, H., Carvalho, F., and Kapur, M. 2024. JABBA: Just Another Bayesian Biomass Assessment. Available from https://github.com/jabbamodel/JABBA.

Winker, H., Carvalho, F., Thorson, J.T., Kell, L.T., Parker, D., Kapur, M., Sharma, R., Booth, A.J., and Kerwath, S.E. 2020. JABBA-Select: Incorporating life history and fisheries' selectivity into surplus production models. Fish. Res. **222**: 105355. doi:10.1016/j.fishres.2019.105355.

Xu, H., Thorson, J.T., and Methot, R.D. 2020. Comparing the performance of three data-weighting methods when allowing for time-varying selectivity. Can. J. Fish. Aquat. Sci. **77**(2): 247–263. doi:10.1139/cjfas-2019-0107.

Fig. 1: Estimated trophic level (y-axis) and pelagic proportions (x-axis) for the eastern Bering Sea case study (top panel) or the simulation experiment (bottom panel). Taxa are labeled alphabetically following their row-order in Table S3 and S4, respectively, with vertex circles having size representing the log-mass of each variable, and the edges color-coded to represent the log-consumption flowing from predator to prey. We compute "Pelagic proportion" by treating "Pelagic prod." and "Producer" as the source of pelagic production in each model, respectively.

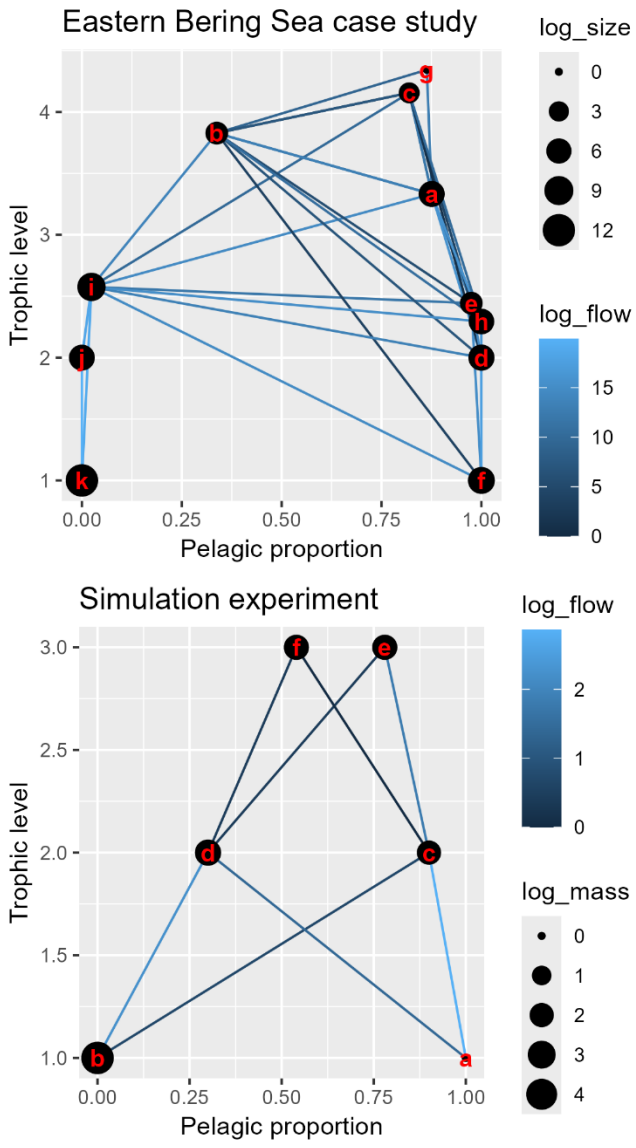

Fig. 2 – Estimated abundance (y-axis in teragrams a.k.a. million metric tons, black line) +/- one standard error (grey shaded ribbon) in each year (x-axis) for each modeled variable (panels), plotted against the indices of biomass (black dots) for cod, arrowtooth, northern fur seals, Pollock, Copepods, Other Zooplankton, Krill, and Primary producers. For pollock, we also show the raw index of biomass (x-symbols) and the index divided by the estimated catchability coefficient (black dots), to show the estimated biomass relative to the bottom-trawl survey scale. Note that Benthic invertebrates, Benthos, and Detritus have neither absolute nor relative abundance available.

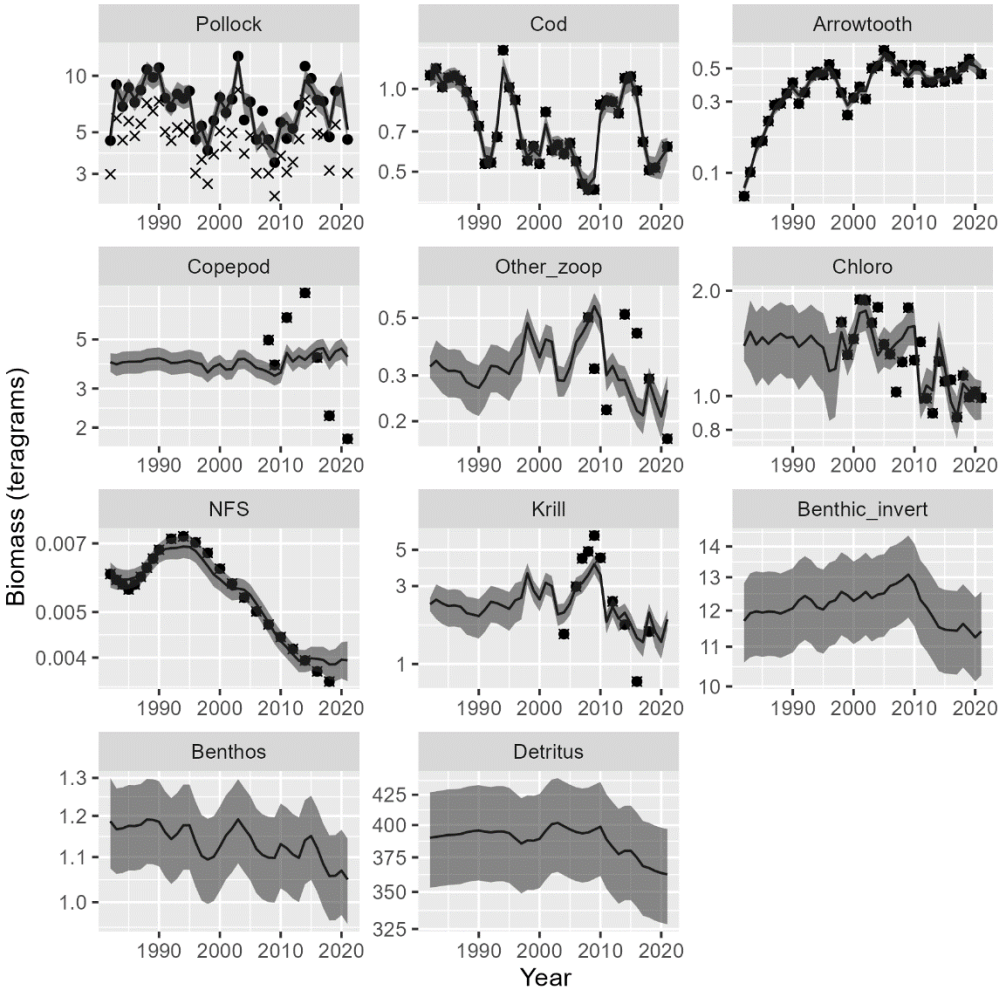

Fig. 3: Comparison of biomass estimates using the full model (black), a null model without process errors or catches (red), a "priors" model that estimates productivity per biomass p_s and consumption per biomass w_s for selected species using a lognormal prior (orange), and a "measurement-error" model that includes catches but no process errors (blue), where each shows +/- one standard error as shading, as well as a comparable stock-assessment estimate of male and female biomass where available (black dotted lines). Note that the "full" and "priors" models are nearly identical (and therefore difficult to distinguish) for cod and arrowtooth.

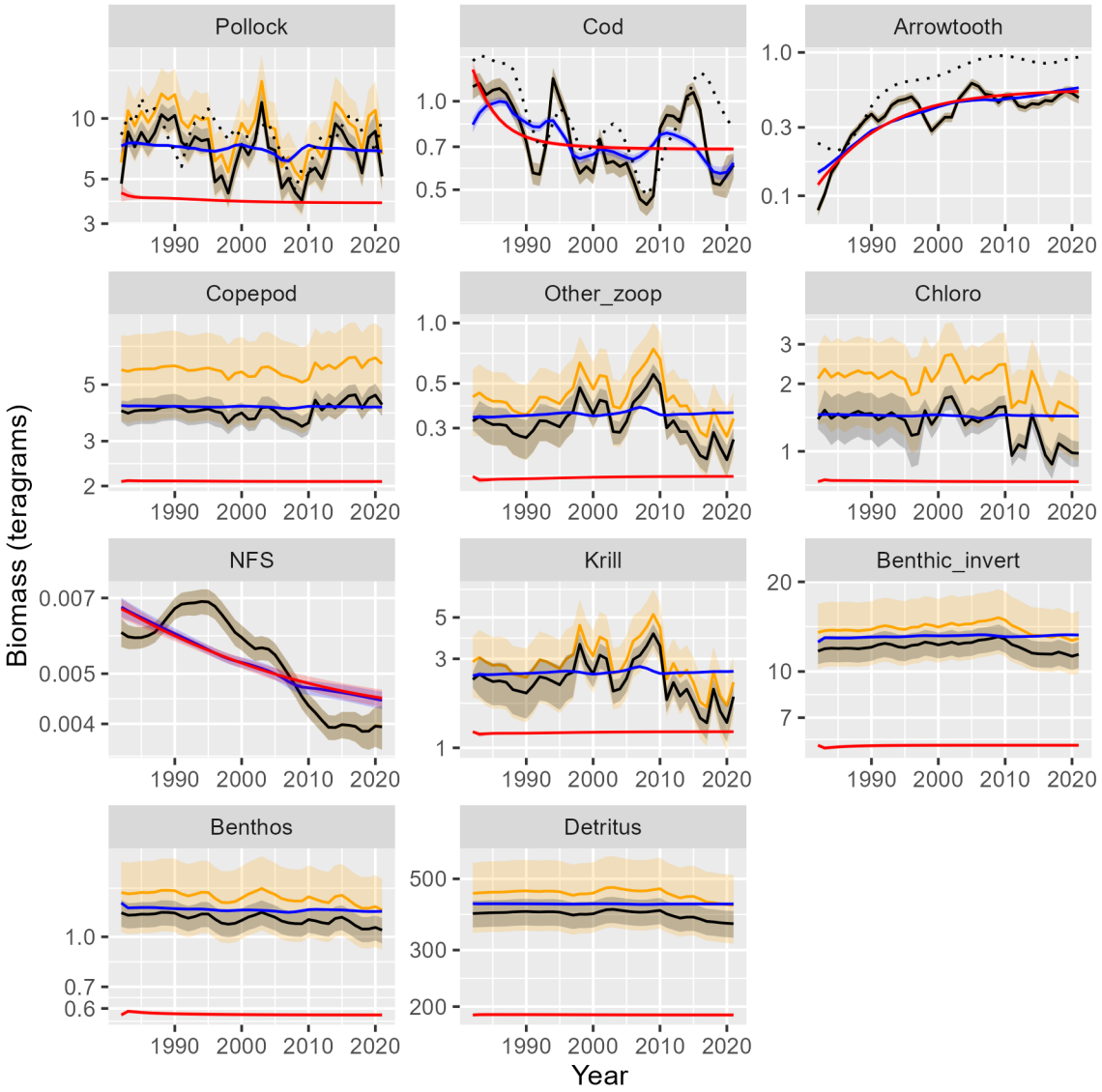

914

Fig. 4 – Estimated rates that affect productivity, i.e., $g(t)$ (production rate; green) and $m(t)$ (mortality rate including consumption; blue) for each modeled species in the eastern Bering Sea using the "full" model, as well as $f(t)$ (fishing mortality rate; red) for the three species with fishery catches, showing the predicted value (line) +/- 1 standard error (shaded area). Note that change in biomass $\frac{d}{dt}\beta(t) = \big(g(t) - f(t) - m(t) + \epsilon(t)\big) \times \beta(t)$ (where process error ϵ is plotted separately in Fig. S2) such that g has a positive effect while m and f have negative effects

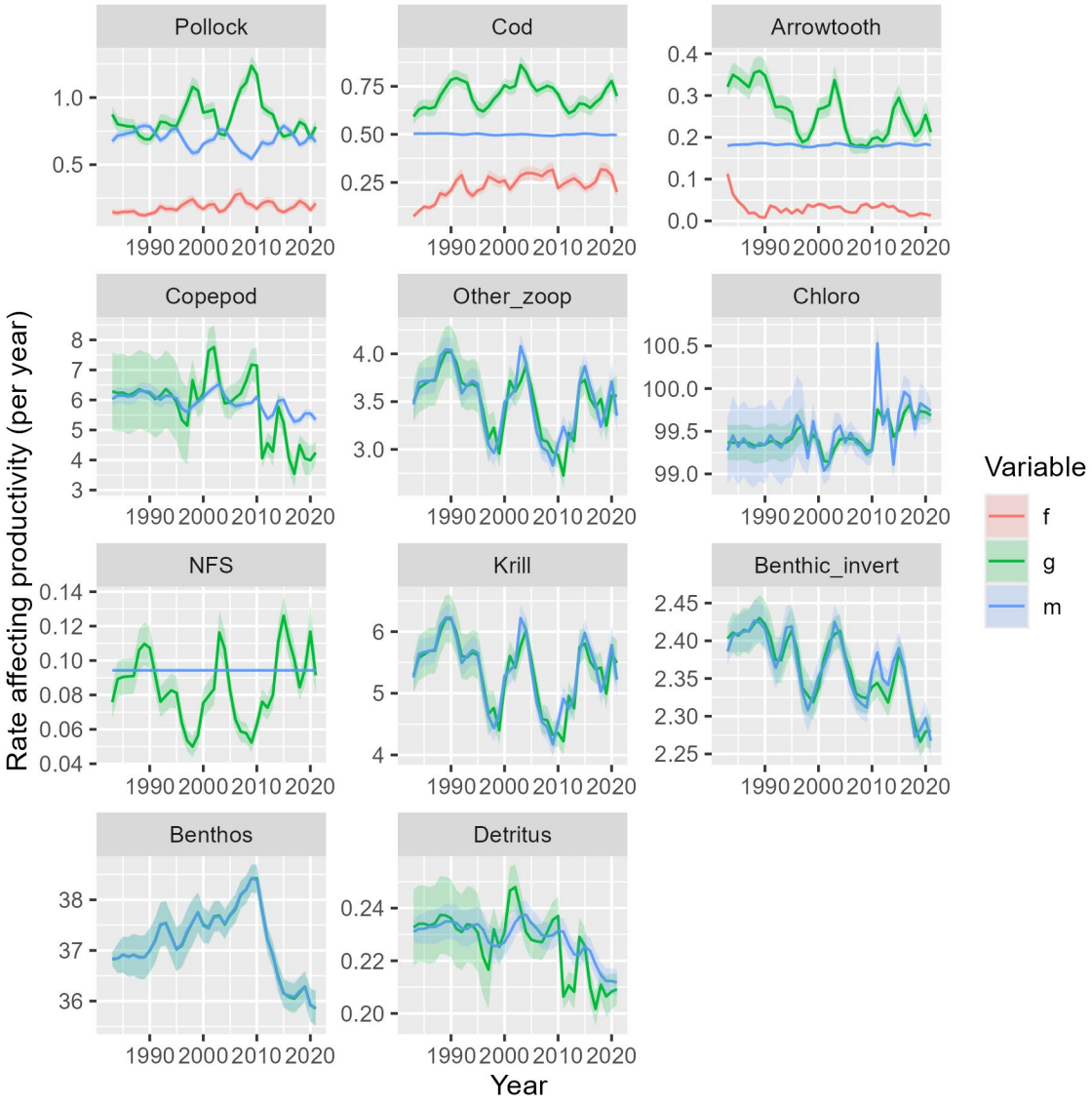

Fig. 5 – Stacked barplot showing growth rate $g(t)$ (left column) or natural mortality rate $m(t)$ (right column) using the "full" model for pollock (top row, i.e., matching green and blue lines in first panel of Fig. 3), cod (middle row, i.e., second panel of Fig. 3), and krill (bottom row, i.e., 8th panel of Fig. 3), while decomposing these demographic rates into the contribution for each prey species (i.e., each component of Eq. 5 for Growth) or for each predator species as well as a constant residual mortality rate (i.e., each component of Eq. 6 for Natural mortality), where $M0$ (pink) indicates residual natural mortality.

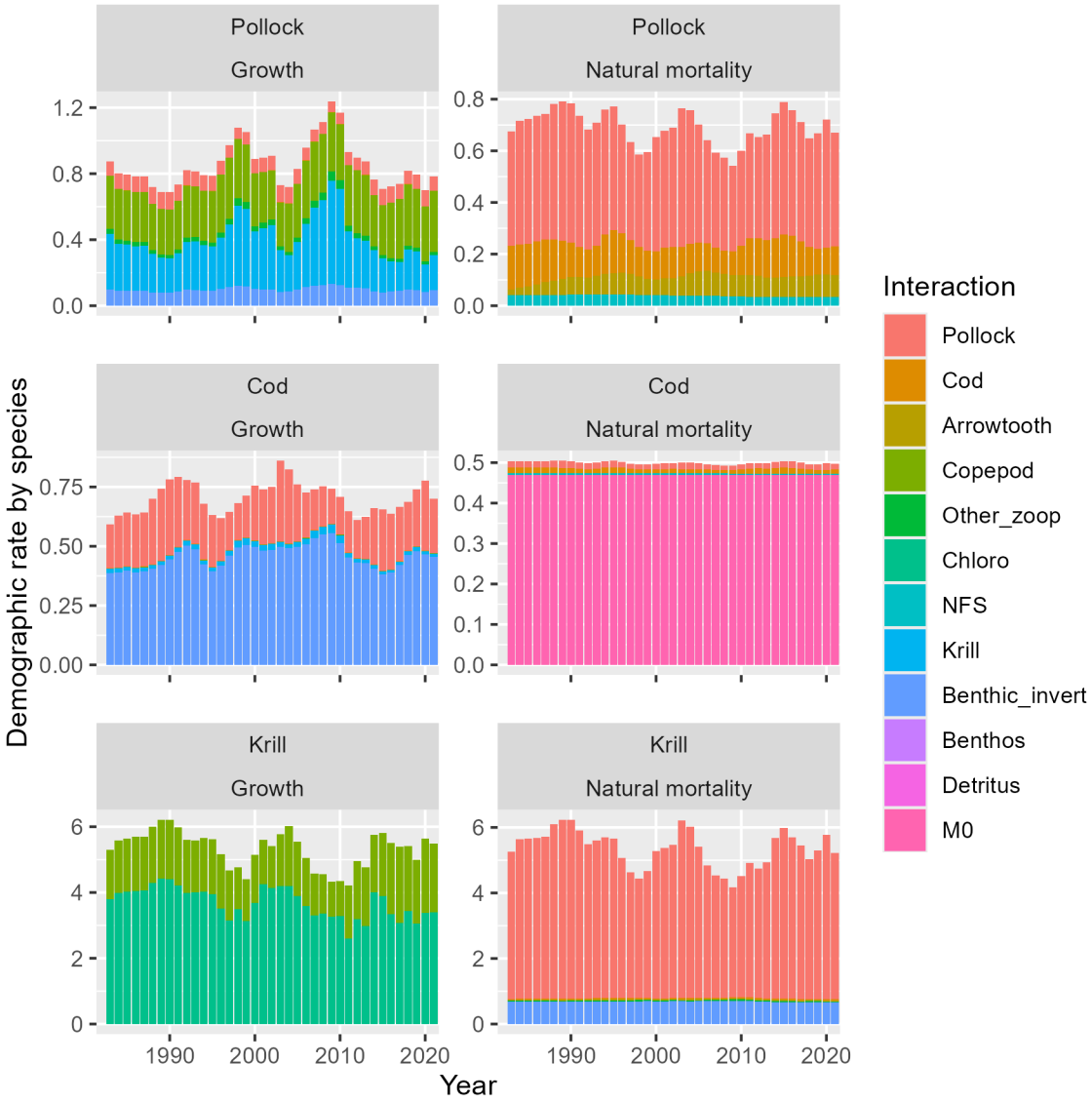

Fig. 6 – Range of errors that covers 10% and 90% of the 50 simulation replicates (y-axis) for each year (x-axis) in annual estimates of growth from consumption (g), mortality due to predation (m) (columns), or biomass (β) for each simulated species (rows) for either the state-space model (red shading) or the same model but without estimating process errors in dynamics (blue shading), and also showing the median error for both models (red and blue lines, respectively). Note that the two predators (bottom two rows) experience no predation (see Table S3) such that their mortality is specified without error and therefore not shown.

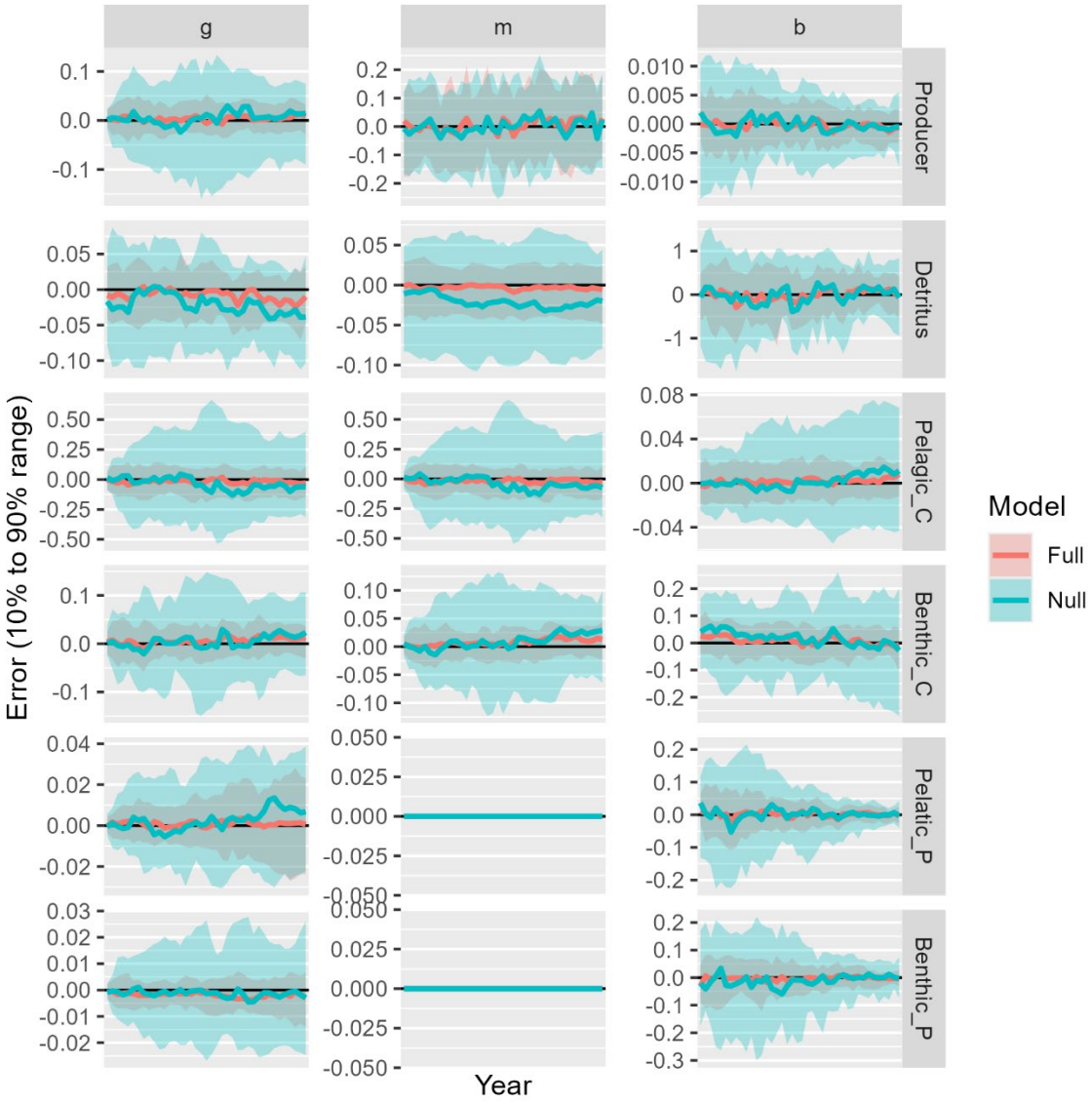

Supplementary Materials 1: Simplifying functional responses

In the main text, we present a formula for consumption (Eq. 4) that eliminates additional terms that can be used to represent ecological interactions among predators and prey. We follow default settings from Rpath (described in Lucey et al. (2020)), and only eliminate terms that are not used given those default values. Here, we summarize how Eq. 4 results from the default values used for these additional terms:

1. *Foraging time:* Ecosim can be configured to represent prey-specific foraging time. Lucey et al. (2020) defines prey-specific foraging time $Ftime_{i,m}$ (see Eq. 19-22 of that paper) and an adjustment rate $Fadj_i$. Their default is to start $Ftime_{i,m} = 1$ in the initial time, with adjustment rate $Fadj_i = 0$, such that $Ftime_{i,m} = 1$ for all subsequent times. As a result, prey-specific foraging time is constant, and this specification avoids integrating additional state variables. Lucey et al. (2020) states that the EwE software uses a default value of $Fadj_i = 0.5$, so EcoState does not correspond to the default values for the EwE software.
2. *Forcing functions*: Ecosim can be configured to include forcing functions, which represent unmodeled variation in consumption. We instead assume that these are captured in estimated process errors, and do not include the option in our definition of consumption.
3. *Prey functional response*: Ecosim can be configured to represent the prey functional response (third term of the right-hand-side of Eq. 4) using a parameter representing predator-specific handling time that controls the shape of the functional response. We again refer to notation from Lucey et al. (2020 Eq. 19-22), which defines predator-specific handling time parameter D_{ij} (which accounts for predator saturation as prey become abundant), and functional-response parameter θ ($\theta = 1$ results in a Holling's Type-2 and $\theta = 2$ results in a

Holling's Type-3 functional response). Their default is $D_{ij} = 1000$ and $\theta = 1$, and they note that "for practical use, values $D_{ij} > 1000$ are indistinguishable from infinity" for parameter D_{ij}. We therefore instead define $D_{ij} \to \infty$, where these values for D_{ij} and θ then simplify to the linear prey functional response that is included in the main text.

4. *Facilitation and multispecies functional response:* Ecosim includes parameters that control whether consumption for a given pair of predator and prey is affected the biomass of other predators or prey. This then represents e.g., facilitation or interference competition. Default values from Lucey et al. (2020) eliminate those responses, so we do not include them in Eq. 4 notation.

We recommend that future research explore the costs (e.g., computational time), benefits (e.g., ecological realism and stability), and trade-offs (e.g., statistical parsimony) that arise when adding these back in.

Works cited

Aydin, K., Gaichas, S., Ortiz, I., Kinzey, D., & Friday, N. (2007). *A comparison of the Bering Sea, Gulf of Alaska, and Aleutian Islands large marine ecosystems through food web modeling* (NOAA Tech. Memo. NMFS-AFSC-178; p. 298). U.S. Dep. Commer. https://repository.library.noaa.gov/view/noaa/22894/noaa_22894_DS1.pdf

Barbeaux, S., Barnett, Lewis, Hall, Madison, Hulson, Pete, Nielsen, Julie, Shotwell, S. Kalei, Siddon, Elizabeth, Spies, Ingrid, & Thorson, James. (2024). *2. Assessment of the Pacific cod stock in the Eastern Bering Sea*. North Pacific Fishery Management Council.

Barbeaux, S. J., Barnett, L., Connor, J., Nielson, J., Shotwell, S. K., Siddon, E., Spies, I., Ressler, H. R., Rohan, S., & Sweeney, K. (2022). Assessment of the Pacific cod stock in the Eastern Bering Sea. *Stock Assessment and Fishery Evaluation Report for the Groundfish Resources of the Bering Sea and Aleutian Islands. North Pacific Fishery Management Council*, *1007*. https://apps-afsc.fisheries.noaa.gov/plan_team/2022/EBSpcod.pdf

Barlow, J., & Boveng, P. (1991). MODELING AGE-SPECIFIC MORTALITY FOR MARINE MAMMAL POPULATIONS. *Marine Mammal Science*, *7*(1), 50–65. https://doi.org/10.1111/j.1748-7692.1991.tb00550.x

Brown, Z. W., Dijken, G. L. van, & Arrigo, K. R. (2011). A reassessment of primary production and environmental change in the Bering Sea. *Journal of Geophysical Research: Oceans*, *116*(C8). https://doi.org/10.1029/2010JC006766

Choquet, M., Kosobokova, K., Kwaśniewski, S., Hatlebakk, M., Dhanasiri, A. K. S., Melle, W., Daase, M., Svensen, C., Søreide, J. E., & Hoarau, G. (2018). Can morphology reliably

distinguish between the copepods Calanus finmarchicus and C. glacialis, or is DNA the only way? *Limnology and Oceanography: Methods*, *16*(4), 237–252. https://doi.org/10.1002/lom3.10240

Edwards, A. M., & Auger-Méthé, M. (2019). Some guidance on using mathematical notation in ecology. *Methods in Ecology and Evolution*, *10*(1), 92–99. https://doi.org/10.1111/2041-210X.13105

Frost, B. W. (1974). Calanus marshallae, a new species of calanoid copepod closely allied to the sibling species C. finmarchicus and C. glacialis. *Marine Biology*, *26*(1), 77–99. https://doi.org/10.1007/BF00389089

Ianelli, J. N., Honkalehto, T., Wassermann, Sophia, Lauffenburger, Nathan, McGilliard, Carey, & Siddon, E. (2023). *Assessment of the walleye pollock stock in the Eastern Bering Sea* [NPFMC Bering Sea and Aleutian Islands SAFE]. North Pacific Fishery Management Council.

Ianelli, J. N., Stienessen, S., Honkalehto, T., Siddon, E., & Allen-Akselrud, C. (2022). *Assessment of the walleye pollock stock in the Eastern Bering Sea* [NPFMC Bering Sea and Aleutian Islands SAFE]. North Pacific Fishery Management Council.

Incze, L. S., Siefert, D. W., & Napp, J. M. (1997). Mesozooplankton of Shelikof Strait, Alaska: Abundance and community composition. *Continental Shelf Research*, *17*(3), 287–305. https://doi.org/10.1016/S0278-4343(96)00036-2

Kimmel, D. G., & Duffy-Anderson, J. T. (2020). Zooplankton abundance trends and patterns in Shelikof Strait, western Gulf of Alaska, USA, 1990–2017. *Journal of Plankton Research*, *42*(3), 334–354. https://doi.org/10.1093/plankt/fbaa019

Livingston, P. A., Aydin, K., Buckley, T. W., Lang, G. M., Yang, M.-S., & Miller, B. S. (2017). Quantifying food web interactions in the North Pacific – a data-based approach. *Environmental Biology of Fishes*, *100*(4), 443–470. https://doi.org/10.1007/s10641-017-0587-0

Lucey, S. M., Gaichas, S. K., & Aydin, K. Y. (2020). Conducting reproducible ecosystem modeling using the open source mass balance model Rpath. *Ecological Modelling*, *427*, 109057. https://doi.org/10.1016/j.ecolmodel.2020.109057

Maritorena, S., d'Andon, O. H. F., Mangin, A., & Siegel, D. A. (2010). Merged satellite ocean color data products using a bio-optical model: Characteristics, benefits and issues. *Remote Sensing of Environment*, *114*(8), 1791–1804.

Markowitz, E. H., Dawson, E. J., Charriere, N. E., Prohaska, B. K., Rohan, S. K., Stevenson, D. E., & Britt, L. L. (2022). *Results of the 2021 eastern and northern Bering Sea continental shelf bottom trawl survey of groundfish and invertebrate fauna*. https://repository.library.noaa.gov/view/noaa/47710

McHuron, E.A., Luxa, K., Pelland, N.A., Holsman, K., Ream, R.R., Zeppelin, T.K., & Sterling J.T. (2020). Practical Application of a Bioenergetic Model to Inform Management of a Declining Fur Seal Population and Their Commercially Important Prey. *Frontiers in Marine Science*. https://doi.org/10.3389/fmars.2020.597973

Miller, C. B. (1988). *Neocalanus flemingeri*, a new species of Calanidae (Copepoda: Calanoida) from the subarctic Pacific Ocean, with a comparative redescription of *Neocalanus plumchrus* (Marukawa) 1921. *Progress in Oceanography*, *20*(4), 223–273. https://doi.org/10.1016/0079-6611(88)90042-0

Napp, Jeffrey. M., Incze, L. S., Ortner, P. B., Siefert, D. L. W., & Britt, L. (1996). The plankton of Shelikof Strait, Alaska: Standing stock, production, mesoscale variability and their

relevance to larval fish survival. *Fisheries Oceanography*, *5*(s1), 19–38. https://doi.org/10.1111/j.1365-2419.1996.tb00080.x

Polovina, J. J. (1984). Model of a coral reef ecosystem. *Coral Reefs*, *3*(1), 1–11. https://doi.org/10.1007/BF00306135

Ressler, P. H., De Robertis, A., Warren, J. D., Smith, J. N., & Kotwicki, S. (2012). Developing an acoustic survey of euphausiids to understand trophic interactions in the Bering Sea ecosystem. *Deep Sea Research Part II: Topical Studies in Oceanography*, *65–70*, 184–195. https://doi.org/10.1016/j.dsr2.2012.02.015

Shotwell, S. K., Bryan, Meaghan, Hanselman, Dana H., Markowitz, Emily, Siddon, Elizabeth, Spies, Ingrid, & Sullivan, Jane. (2023). *Assessment of the arrowtooth flounder stock in the Bering Sea and Aleutian Islands*. North Pacific Fishery Management Council. https://apps-afsc.fisheries.noaa.gov/Plan_Team/2023/BSAIatf.pdf

Shotwell, S. K., Spies, I., Brit, L., Bryan, M., Hanselman, D. H., Nichol, D. G., Hoff, J., Palsson, W., Siwicke, K., & Wilderbuer, T. K. (2021). Assessment of the arrowtooth flounder stock in the Bering Sea and Aleutian Islands. *Stock Assessment and Fishery Evaluation Report for the Groundfish Resources of the Bering Sea and Aleutian Islands. North Pacific Fishery Mngt. Council, Anchorage, AK*, *99501*. https://apps-afsc.fisheries.noaa.gov/Plan_Team/2023/BSAIatf.pdf

Siler, W. (1979). A Competing-Risk Model for Animal Mortality. *Ecology*, *60*(4), 750–757. https://doi.org/10.2307/1936612

Sullaway, G. (In revisions). *Evaluating the Performance of a System Model in Predicting Zooplankton Dynamics: Insights from the Bering Sea Ecosystem*.

Tarrant, A. M., Eisner, L. B., & Kimmel, D. G. (2021). Lipid-related gene expression and sensitivity to starvation in Calanus glacialis in the eastern Bering Sea. *Marine Ecology Progress Series*, *674*, 73–88. https://doi.org/10.3354/meps13820

Trites, A. W., & Bigg, M. A. (1996). Physical growth of northern fur seals (Callorhinus ursinus): Seasonal fluctuations and migratory influences. *Journal of Zoology*, *238*(3), 459–482. https://doi.org/10.1111/j.1469-7998.1996.tb05406.x

Walters, C., Christensen, V., & Pauly, D. (1997). Structuring dynamic models of exploited ecosystems from trophic mass-balance assessments. *Reviews in Fish Biology and Fisheries*, *7*(2), 139–172. https://doi.org/10.1023/A:1018479526149

Whitehouse, G. A., Aydin, K. Y., Hollowed, A. B., Holsman, K. K., Cheng, W., Faig, A., Haynie, A. C., Hermann, A. J., Kearney, K. A., Punt, A. E., & Essington, T. E. (2021). Bottom–Up Impacts of Forecasted Climate Change on the Eastern Bering Sea Food Web. *Frontiers in Marine Science*, *8*. https://doi.org/10.3389/fmars.2021.624301

Wiebe, P. H. (1975). Relationships between zooplankton displacement volume, wet weight, dry weight and carbon. *Fish. Bull.*, *73*, 777–786.

Wiebe, P. H. (1988). Functional regression equations for zooplankton displacement volume, wet weight, dry weight, and carbon: A correction. *Fisheries Bulletin*, *86*, 833–835.

Supplementary Materials 2: Solving for scale for each taxon

For each taxon s, the user must choose whether to treat equilibrium biomass $\bar{\beta}_s$ or ecotrophic efficiency e_s as a parameter for that taxon. A different choice can be made for each taxon, and EcoState then solves for the unspecified value for each taxon (e.g., solves for e_s if $\bar{\beta}_s$ is specified for taxon s). The user can specify one (but not both) of $\bar{\beta}_s$ and e_s for any single taxon, and at least one taxon must have $\bar{\beta}_s$ to avoid a degenerate solution of $\overline{\boldsymbol{\beta}} = \mathbf{0}$ (Polovina, 1984). This algorithm is included in Rpath (Lucey et al., 2020), but we repeat it here using notation from EcoState for readers who are not familiar with the algorithm.

Specifically, we define indicator a_s as:

$$a_s = \begin{cases} 0 & \text{if } \beta_s \text{ is specified} \\ 1 & \text{if } e_s \text{ is specified} \end{cases}$$

such that EcoState will treat $\overline{\boldsymbol{\beta}}_{\{\mathbf{a}=0\}}$ and $\mathbf{e}_{\{\mathbf{a}=1\}}$ as specified values and will solve for the value of $\overline{\boldsymbol{\beta}}_{\{\mathbf{a}=1\}}$ and $\mathbf{e}_{\{\mathbf{a}=0\}}$. We first calculate consumption $\tilde{c}_i$ for each prey i given any specified values of $\bar{\beta}_j$ for predators j:

$$\tilde{c}_i = \sum_{j \in \{\mathbf{a}=1\}} \beta_j d_{i,j}$$

We next define a vector that includes all specified values multiplied by production per biomass, $\mathbf{x} = \mathbf{p} \odot \left((\mathbf{1} - \mathbf{a}) \odot \overline{\boldsymbol{\beta}} + \mathbf{a} \odot \mathbf{e}\right)$, and define the matrix of prey-consumption-per-predator biomass for those species where ecotrophic efficiency is specified, $\mathbf{Z} = \mathbf{D} \odot (\mathbf{1}\mathbf{w}^T) \odot (\mathbf{1}\mathbf{a}^T)$. We seek to solve for the unspecified values $\mathbf{y} = \mathbf{a} \odot \overline{\boldsymbol{\beta}} + (\mathbf{1} - \mathbf{a}) \odot \mathbf{e}$. To do so, we calculate:

$$\mathbf{y} = (\mathrm{diag}(\mathbf{x}) - \mathbf{Z})^{-1}\tilde{\mathbf{c}}$$

where $\mathrm{diag}(\mathbf{x})$ is a diagonal matrix with diagonal elements of $\mathbf{x}$. We then plug $\mathbf{y}$ into the unknown values, $\overline{\boldsymbol{\beta}}_{\{\mathbf{a}=1\}} = \mathbf{y}_{\{\mathbf{a}=1\}}$ and $\mathbf{e}_{\{\mathbf{a}=0\}} = \mathbf{y}_{\{\mathbf{a}=0\}}$.

Supplementary Materials 3: Data standardization

Zooplankton Sampling and Data Processing

Zooplankton was collected using oblique tows of paired bongo nets (20 cm frame, 153 μm mesh and 60 cm frame, 333 or 505 μm mesh) (Incze et al., 1997; Napp et al., 1996). The tows were within 5-10 m of the bottom depending on sea state and depth was monitored continuously using a SeaBird FastCAT CTD. Volume filtered was estimated using a General Oceanics flowmeter mounted inside the mouth of each net. Samples were preserved in 5% buffered formalin/seawater. Whole sample displacement volumes were estimated by first concentrating all animals onto a sieve using a small mesh size (53 μm) and all water was allowed to drain from the sieve. The animals are then added to a graduated cylinder of known volume and the difference in volume was recorded in mL. Zooplankton were identified to the lowest taxonomic level and stage possible at the Plankton Sorting and Identification Center in Szczecin, Poland, and verified at the Alaska Fisheries Science Center, Seattle, Washington, USA. A methodological change in zooplankton collection occurred in 2012, when the 60 cm frame net had its mesh changed to 505 μm. The majority of taxa were not affected by this change; however, the potential for some differences to arise were noted, see Kimmel and Duffy-Anderson (2020) for details.

Biomass was estimated for whole samples by converting the displacement volume (mL) to biomass using literature equations (Wiebe et al. 1975, Wiebe 1988). Biomass estimates for individual species were calculated from abundance (ind m^{-3}) estimates. Individual stage weight (wet mass) was estimated from laboratory measurements for *Calanus marshallae/glacialis*, *Neocalanus* spp. (*N. plumchrus* and *N. flemingeri* combined), and *N. cristatus* (Hopcroft unpub.) (Sullaway, In revisions). Note that the ability to distinguish between these *Calanus* species

morphologically is based on taxonomic characters that require significant processing time (Frost, 1974). This appears to be a problem across the genus as it has been suggested that the ability to distinguish between *C. glacialis* and *C. finmarchicus* in Atlantic waters can only be accomplished with DNA methods (Choquet et al., 2018). Recent results suggest that most *Calanus* spp. in the Bering Sea may in fact be *C. glacialis* (Tarrant et al., 2021). Similarly, *N. flemingeri* and *N. plumchrus* are closely related species in both size and mass (Miller, 1988); therefore, these two species were not distinguished in this analysis. Individual masses for the following stages were then summed for each sampling event to produce a single biomass estimate for copepodite stages C1-C6, with C6 being the adult stage. Wet mass was converted to dry mass or carbon using literature equations (Wiebe, 1975, 1988). Total large copepod biomass was then substracted from the whole sample biomasses to remove that contributing fraction to produce the large copepod and the other zooplankton biomass time-series.

Northern Fur Seals

Northern fur seal pups have been routinely counted on the Pribilof Islands (St. Paul Island, St. George Island) since the 1950s. From 1982 to 1992, pup counts were largely conducted annually on St. Paul Island and biennially on St. George Island, whereas from 1992 onwards they were largely biennial on both islands. Counts of the entire population are not possible because at any given time a certain proportion of the population is at sea. The Pribilof Island population has been in decline since the mid-to-late 1990s, primarily driven by declines on St. Paul Island, although it is unknown which component of the population is driving the decline. To estimate population size, we used the modeling approach described in McHuron et al. (2020), which resulted in a total of 11 different estimates of numbers at age for male and female fur seals. Animals <2 years of age were not included in population estimates since pups predominately rely

on milk from their mother while in the eastern Bering Sea, and once they depart on their post-weaning migration, most pups do not return until two years of age. See Supplementary Text in McHuron et al. (2020) for a more complete description. Population biomass in each year was estimated by multiplying the numbers at age for each sex (averaged across all 11 models) with age-sex specific mass estimates (Trites & Bigg, 1996) and then summing across all age and sex classes. The resulting population estimate was multiplied by ca. 30% to account for the fact that fur seals are seasonal residents of the eastern Bering Sea, spending on average of 105 - 109 days foraging in the model area. We only used biomass estimates from years where empirical estimates of pup production were available.

Ecopath parameters

Estimates of production per biomass (p_s and called P/B elsewhere), consumption per biomass (w_s and called Q/B elsewhere), and diet composition were derived from previous Ecopath with Ecosim models for the eastern Bering Sea. Detailed parameter estimation methods for all EBS EwE functional groups can be found in Aydin et al. (2007). Specifically:

- *Groundfish groups* combined mortality estimates from the literature and stock assessments with growth information available from field studies or the literature. Groundfish diet compositions were obtained from the NOAA/AFSC groundfish food habits monitoring program (Livingston et al., 2017). The groundfish diet compositions were combined across predator size classes by taking the weighted average of age-specific consumption, weighted by the product of abundance-at-age from stock assessments, size-at-age from assumed growth functions, and ration-at-size from bioenergetic models.
- *Northern fur seal* production was estimated with Siler's (1979) competing risk model as modified by Barlow and Boveng (1991) to construct a general model of survivorship. The

1176 northern fur seal diet composition was compiled from the literature. However, we substitute
1177 a bioenergetic calculation for consumption per biomass based on a recently published
1178 bioenergetic model (McHuron unpublished work), which corrected for seasonal residency in
1179 the modeled area;
1180 • *Zooplankton* production rates and diet compositions were estimated from values reported in
1181 the literature. The copepod consumption rate was retrieved from the literature, while the
1182 consumption of euphausiids and other zooplankton was estimated with an assumed growth
1183 efficiency.
1184 • *Benthic invertebrate* production rates were from the literature and consumption was
1185 estimated with an assumed growth efficiency. Estimates of P/B and Q/B for commercial
1186 crabs were derived from stock assessment information. Benthic invertebrate diet
1187 compositions were derived from literature sources. The production of benthic microbes were
1188 derived from literature values for pelagic microbes. The Q/B of benthic microbes was
1189 estimated assuming a growth efficiency of 0.35, and the diet composition was assumed to
1190 consist entirely of detritus.
1191 We then aggregated multiple groups to create the variables used here. This aggregation is done
1192 by taking the biomass-weighted average of production per biomass p_s, consumption per biomass
1193 w_s, and diet proportions $d_{i,j}$ across multiple taxa from Whitehouse et al. (2021). Pollock, cod,
1194 arrowtooth, and northern fur seal all aggregated juvenile and adult stages from Whitehouse et al.
1195 (2021). Similarly, Chloro included large and small phytoplankton, and Benthic_invert included
1196 tanner, snow, and king crabs, pandalid shrimps, benthic zooplankton, motile epifauna, structural
1197 epifauna, and infauna. The biomass variables from Whitehouse et al. (2021) that are aggregated
1198 into our 10 biomass variables (i.e., excluding detritus) represents 79% of the total biomass from

1199 Whitehouse et al. (2021). The diet-composition matrix was then rescaled to ensure that each
1200 predator had proportions that summed to one.
1201
1202 **Primary producers**
1203 Satellite chlorophyll-*a* concentration data from 1998 to 2023 for the southern (<60 N) Bering Sea
1204 middle and outer shelf (50-180 m bottom depth) were used to calculate annual time series trends.
1205 We compiled 8-day satellite chlorophyll-*a* concentration (ug l^{-1}) at a 4 km-resolution from The
1206 Hermes GlobColour website: http://hermes.acri.fr/ (Maritorena et al., 2010). This product is a
1207 standardized merged chlorophyll-*a* product, combining remote sensing data from SeaWiFS,
1208 MERIS, MODIS, VIIRS and OLCI. chlorophyll-*a* concentration data. Data were averaged for
1209 the months May to October for the middle and outer southern Bering Sea shelf region.
1210 Chlorophyll-*a* concentration data from locations near river plumes from the Yukon and
1211 Kuskowim rivers can be highly uncertain and were excluded, following recommendations in
1212 Brown et al. (2011).
1213

Supplementary Materials 4: Additional tables and figures

Table S1: Notation used in the model presentation and results, including the symbol, units, a brief description, and the type. Note that notation differs from past Ecopath-with-Ecosim standards, to avoid using multiple symbols to indicate a single variable (Edwards & Auger-Méthé, 2019).

Symbol	Units	Description	Type
s	-	Species	Index
i	-	Prey	Index
j	-	Predator	Index
t	-	Time index	Index
k	-	Fishery	Index
$h_s(t)$	$Mass$	Catch for each species s and time t	Data
$b_s(t)$	$Mass$	Biomass index	Data
p_s	$Time^{-1}$	Production rate per biomass (elsewhere called PB)	Specified
w_s	$Time^{-1}$	Consumption rate per biomass (elsewhere called QB)	Specified
$x_{i,j}$	$Unitless$	Vulnerability for prey i to predator j (called X_{ij} in Walters et al. (1997))	Specified
$d_{i,j}$	$Unitless$	Diet fraction for prey i and predator j	Specified
$r_{s,f}$	$Unitless$	Selectivity ratio for each species s in a given fishery f	Specified
σ_s^2	$Unitless$	Measurement error variance for biomass indices	Specified
v_s^2	$Unitless$	Measurement error variance for catch data	Specified
$y_s(t)$	$Time^{-1}$	Tracer release for taxa s	Specified
$\bar{\beta}_s$	$Mass$	Equilibrium biomass	Estimated
$\phi_k(t)$	$Time^{-1}$	Annual fishing mortality rate	Estimated
q_s	$Unitless$	Catchability coefficient for species s	Estimated
δ_s	$Unitless$	Difference between biomass and equilibrium biomass in the initial time	Estimated
τ_s^2	$Unitless$	Process error variance for biomass dynamics	Estimated
$\epsilon_s(t)$	$Time^{-1}$	Process error variation	Estimated
$\beta_s(t)$	$Mass$	Modeled biomass	Derived
$\eta_s(t)$	$Mass$	Modeled catch	Derived
$g_s(t)$	$Time^{-1}$	Growth rate	Derived
e_s	$Time^{-1}$	Ecotrophic efficiency	Derived
v_s	$Time^{-1}$	Detritus export (a.k.a. turnover) rate	Derived
u_s	$Time^{-1}$	Unmodeled mortality rate (elsewhere called $M0$)	Derived
$c_{i,j}(t)$	$Time^{-1}$	Consumption for each prey i and predator j	Derived
$\bar{c}_{i,j}$	$Time^{-1}$	Equilibrium consumption	Derived
$g_s(t)$	$Time^{-1}$	Growth rate per biomass	Derived
$m_s(t)$	$Time^{-1}$	Natural mortality rate per biomass	Derived
$f_s(t)$	$Time^{-1}$	Fishing mortality rate per biomass	Derived
$z_s(t)$	$Unitless$	Tracer concentration for predator s	Derived

1220 Table S2: Data sets used for fitting the eastern Bering Sea case study

Data set	Years covered	Details	Reference
Cod, pollock, and arrowtooth biomass	1982-2023 (annual)	Using the design-based biomass index from a summer bottom trawl survey	(Markowitz et al., 2022)
Copepod and Other pelagic zooplankton biomass index	2008, 2009, 2011, 2014, 2016, 2018, 2021, 2022	From an oblique-tow small-mesh pelagic trawl, averaging Spring (May) and Fall (September) densities	(Incze et al., 1997; Kimmel & Duffy-Anderson, 2020)
Primary production biomass index	1998-2023 (annual)	From satellite chlorophyll-*a* concentration measurements, averaged from May through October of each year	
Krill biomass	2004, 2006-2010, 2012, 2014, 2016, 2018, 2022	From summer acoustic-midwater trawl survey	(Ressler et al., 2012)
Northern fur seal biomass	1982-2018 (biennial after 1990)		(McHuron et al., 2020)
Total catch biomass for cod, pollock, and arrowtooth	1982-2023 (annual)	From stock assessments	(S. J. Barbeaux et al., 2022; Ianelli et al., 2022; Shotwell et al., 2021)
Ecopath parameters and diet matrix	NA	From previous Rpath model	(Aydin et al., 2007; Whitehouse et al., 2021)

1221

Table S3: Ecopath parameters (rows) specified or calculated for each taxa (column) in the eastern Bering Sea case study (see Table S1 for units, where $Mass$ is using million metric tons and $Time$ is using years), and also showing diet proportions for prey (rows) given each taxa as predator (columns). Note that cod, arrowtooth, and northern fur seal (NFS) estimate equilibrium biomass $\bar{\beta}_s$ given the assumption that their catchability coefficient $q_s = 1$, and ecotrophic efficiency e_s is calculated to match that value. For other species, we specify ecotrophic efficiency $e_s = 1$ and equilibrium biomass $\bar{\beta}_s$ is calculated to match that value.

		Pollock	Cod	Arrow.	Copepod	Other zoop.	Pelagic prod.	NFS	Krill	Benthic invert	Benthic microbes	Detritus
Parameter or derived quantity	type	hetero	hetero	hetero	hetero	hetero	auto	hetero	hetero	hetero	hetero	detritus
	w_s	4.226	2.745	1.201	27.74	10.19	NA	57.764	15.64	11.912	104.29	NA
	p_s	0.825	0.507	0.186	6	3.57	99.407	0.094	5.48	2.43	36.5	0.5
	$\bar{\beta}_s$	7.186	1.639	0.896	3.95	0.325	1.39	0.005	2.324	11.706	1.186	390.038
	e_s	1	0.073	0.176	1	1	1	0	1	1	1	1
	u_s	0.2	0.2	0.2	0.2	0.2	0.2	0.2	0.2	0.2	0.2	0.2
	Trophic level	3.332	3.828	4.156	2	2.443	1	4.344	2.294	2.576	2	1
	Pelagic prop.	0.876	0.338	0.819	1	0.975	1	0.863	1	0.024	0	0
Prey proportions (d_{s_2,s_1})	Pollock	0.109	0.332	0.8	0	0	0	0.977	0	0	0	0
	Cod	0.001	0.007	0	0	0	0	0.023	0	0	0	0
	Arrowtooth	0.001	0.001	0.004	0	0	0	0	0	0	0	0
	Copepod	0.388	0.001	0	0	0.301	0	0	0.294	0.002	0	0
	Other zoop.	0.033	0	0	0	0.049	0	0	0	0	0	0
	Pelagic prod.	0	0	0	1	0.6	0	0	0.706	0.007	0	0
	NFS	0	0	0	0	0	0	0	0	0	0	0
	Krill	0.357	0.028	0.113	0	0.025	0	0	0	0.011	0	0
	Ben. Invert	0.112	0.632	0.082	0	0.025	0	0	0	0.158	0	0
	Ben. microbe	0	0	0	0	0	0	0	0	0.311	0	0
	Detritus	0	0	0	0	0	0	0	0	0.511	1	0

Table S4: Ecopath parameters in the simulation experiment (see Table S2 caption for details)

		Producer	Detritus	Pelagic consumer	Benthic consumer	Pelagic predator	Benthic predator
Param	Type	auto	detritus	hetero	hetero	hetero	hetero
	w_s	NA	NA	10	4	3	1
	p_s	90	0.5	4	1	0.2	0.1
	$\bar{\beta}_s$	0.11	10.02	0.78	1.33	1	1
	e_s	0.9	0.9	0.9	0.9	0	0
	u_s	0.2	0.2	0.2	0.2	0.2	0.2
	Trophic level	1	1	2	2	3	3
	u_s	9	0.05	0.4	0.1	0.2	0.1
Prey proportions (d_{s_2,s_1})	Producer_1	0	0	0.9	0.3	0	0
	Producer_2	0	0	0.1	0.7	0	0
	Consumer_1	0	0	0	0	0.8	0.4
	Consumer_2	0	0	0	0	0.2	0.6
	Predator_1	0	0	0	0	0	0
	Predator_2	0	0	0	0	0	0

Table S5: List of estimated parameters and standard errors in the eastern Bering Sea case study, listing the parameter name (see definitions in Table S1), the Taxon s, the maximum likelihood estimator, and the standard error

Parameter	Taxon	Estimate	SE
$\log(\delta_s)$	Pollock	-0.416	0.124
	Cod	-0.38	0.159
	Arrowtooth	-2.424	0.267
	NFS	0.27	0.221
$\log(\bar{\beta}_s)$	Cod	0.494	0.123
	Arrowtooth	-0.11	0.247
	NFS	-5.385	0.2
$\log(\tau_s)$	Pollock	-1.128	0.141
	Cod	-1.591	0.148
	Arrowtooth	-1.997	0.192
	Copepod	0.128	0.169
	NFS	-3.259	0.35
$\log(q_s)$	Pollock	-0.412	0.109
	Copepod	0.102	0.104
	Chloro	4.836	0.124
	Other_zoop	1.848	0.098
	Krill	2.098	0.121

Fig. S1 – Simulated time-series (y-axis) for each year (x-axis) of growth $g(t)$ (left column), natural mortality $m(t)$ (middle column), or biomass $\beta(t)$ (right column) for each simulated taxa (rows).

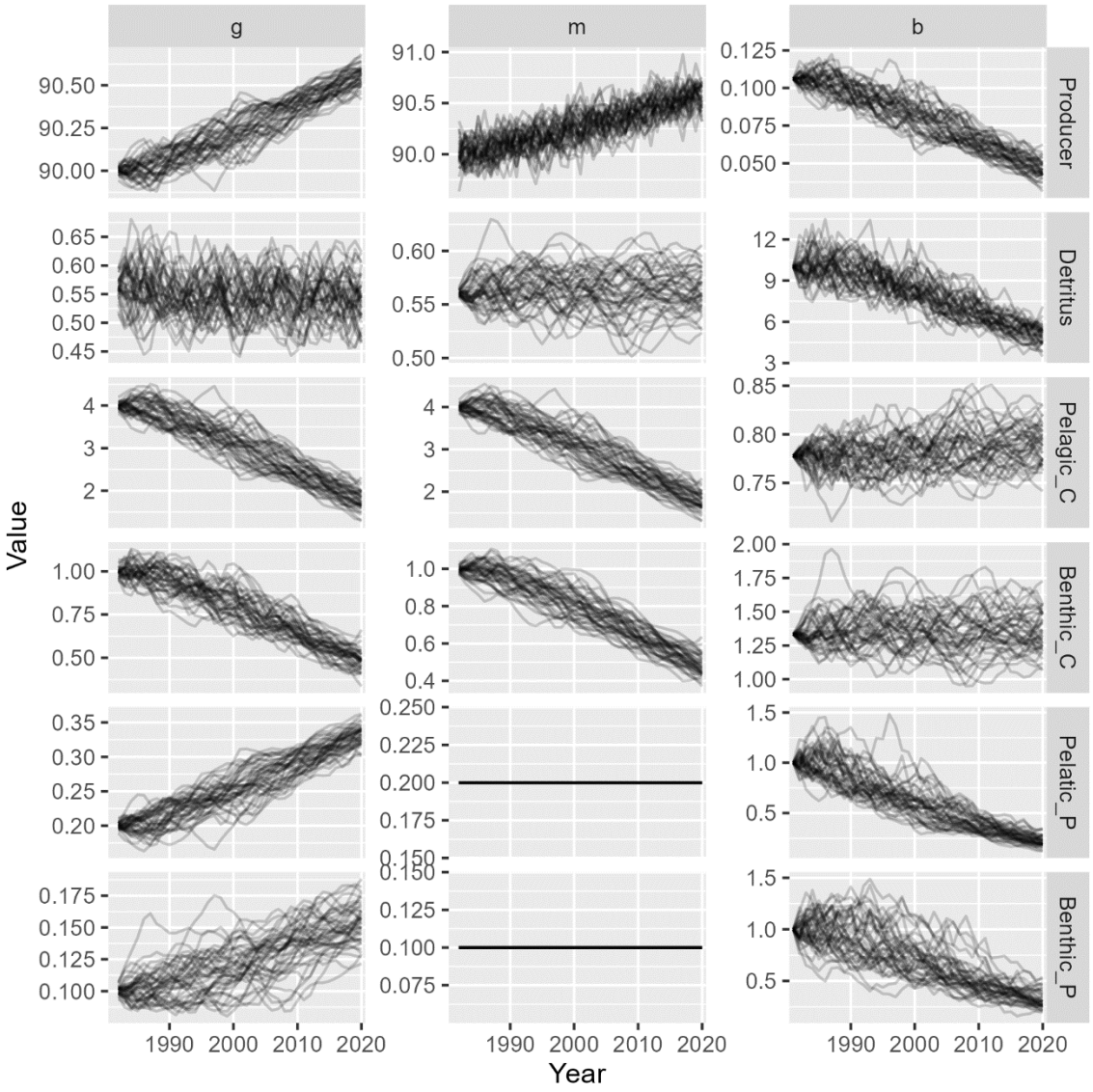

Fig. S2 – Fits to catch data for the three species with a directed fishery, showing predicted $\eta_s(t)$ (black line) +/- 1 standard error (grey shaded area) and observed catch $h_s(t)$ (black bullets).

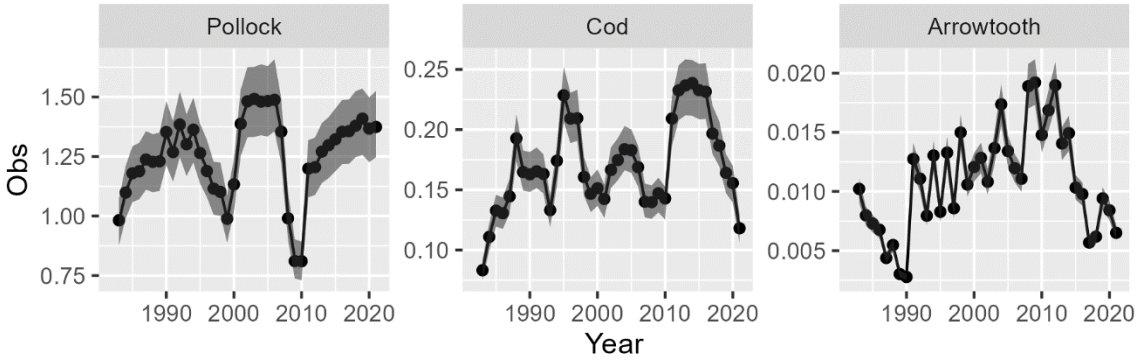

Fig. S3 – Annual estimates of process-error $\epsilon_s(t)$ (black lines) +/- 1 standard error (grey shaded area) for those species for which it is estimated.

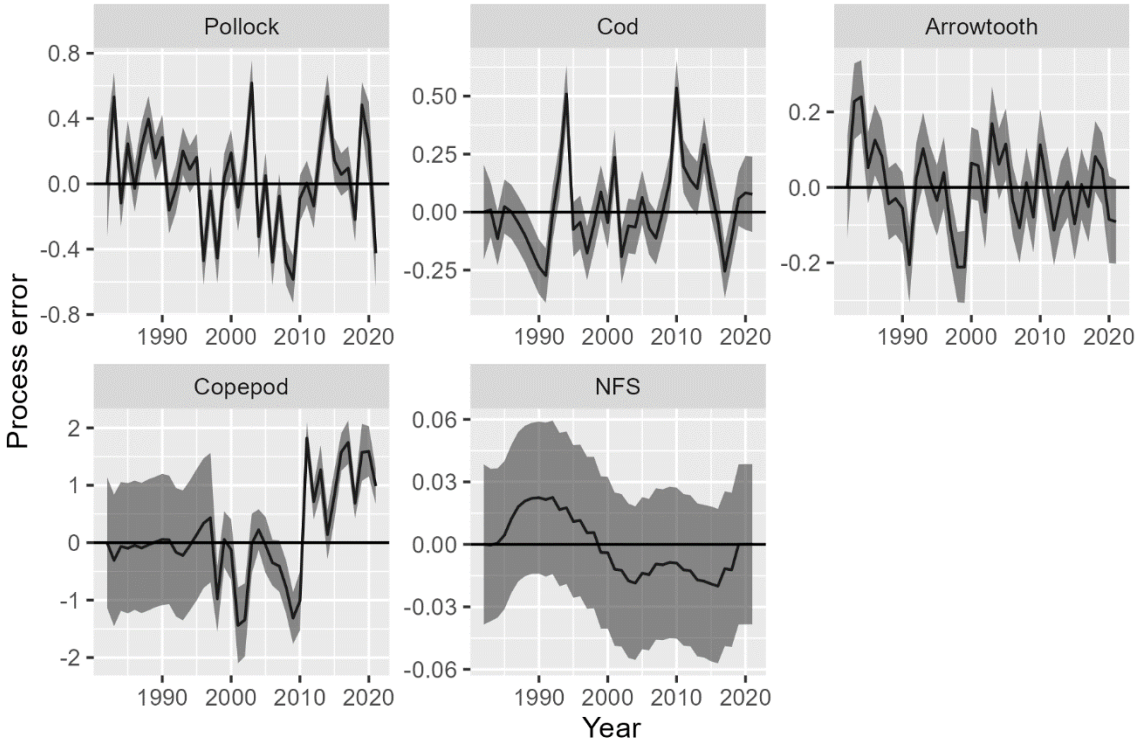

Fig. S4 – Performance (Box: 10% to 90% range; Line: mean) for estimated parameters in the simulation experiment, showing the true value (red), and estimates from the full (green) or null model (blue) for each of 13 parameters, where the single vulnerability parameter x_{shared} represents the predator-prey functional response for all predators and prey, $x_{shared} = 1 + \exp(Xprime\_ij)$ where $Xprime\_ij$ is the estimated parameter with unbounded support, and $Xprime\_ij$ is shown here. Note that the null model does not estimate process errors, and, therefore, has no value listed for the standard deviation of process errors (τ_s).

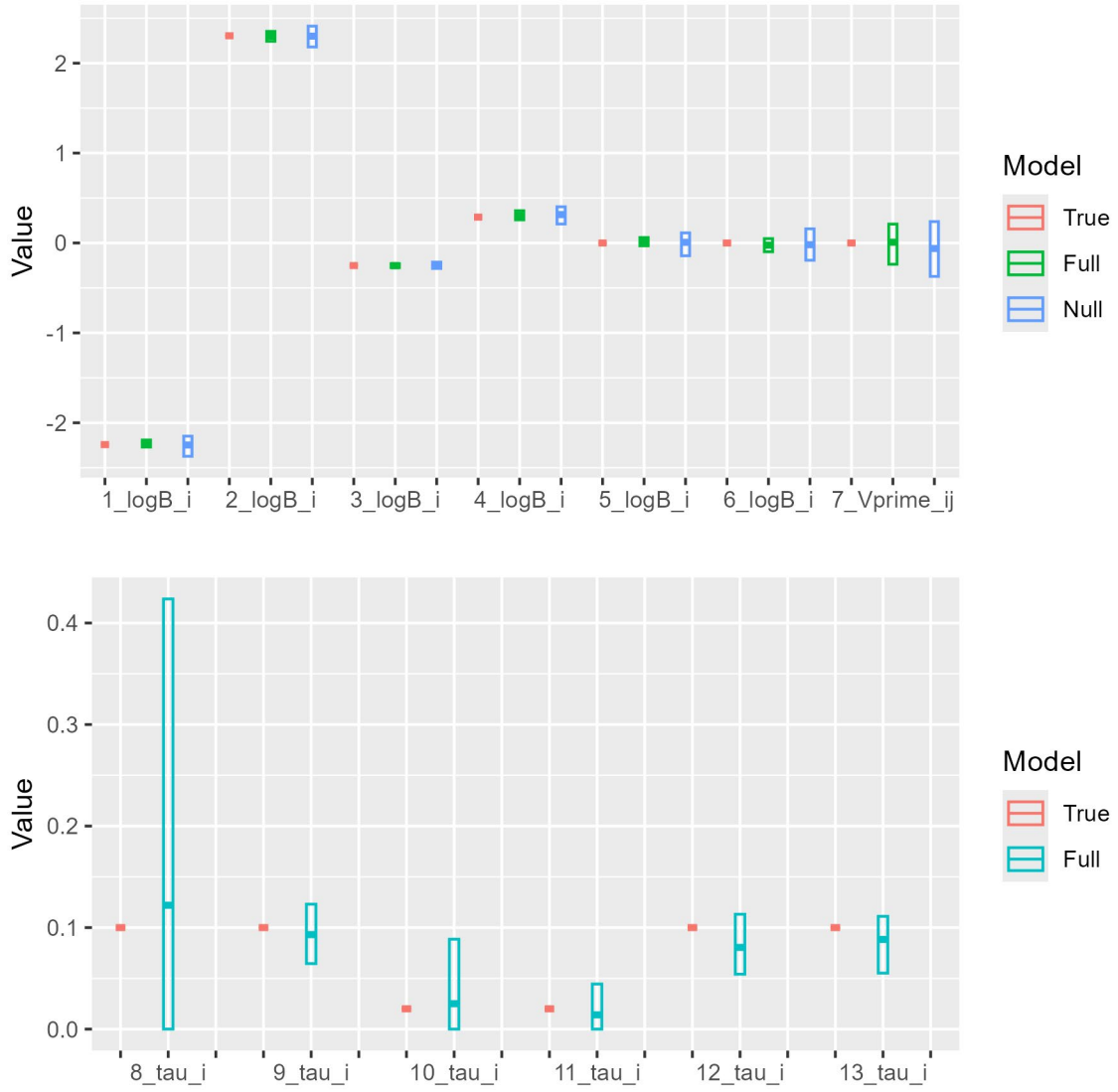

Fig. S5 – Range of errors that covers 10% and 90% of the 50 simulation replicates for each year in annual estimates of growth from consumption (g), mortality due to predation (m), or biomass (β) for each simulated species (see Fig. 6 caption for details), when replicating the simulation experiment while estimating productivity per biomass p_s for all six taxa and consumption per biomass w_s for the consumers and predators using a lognormal prior with a log-standard deviation of 0.1

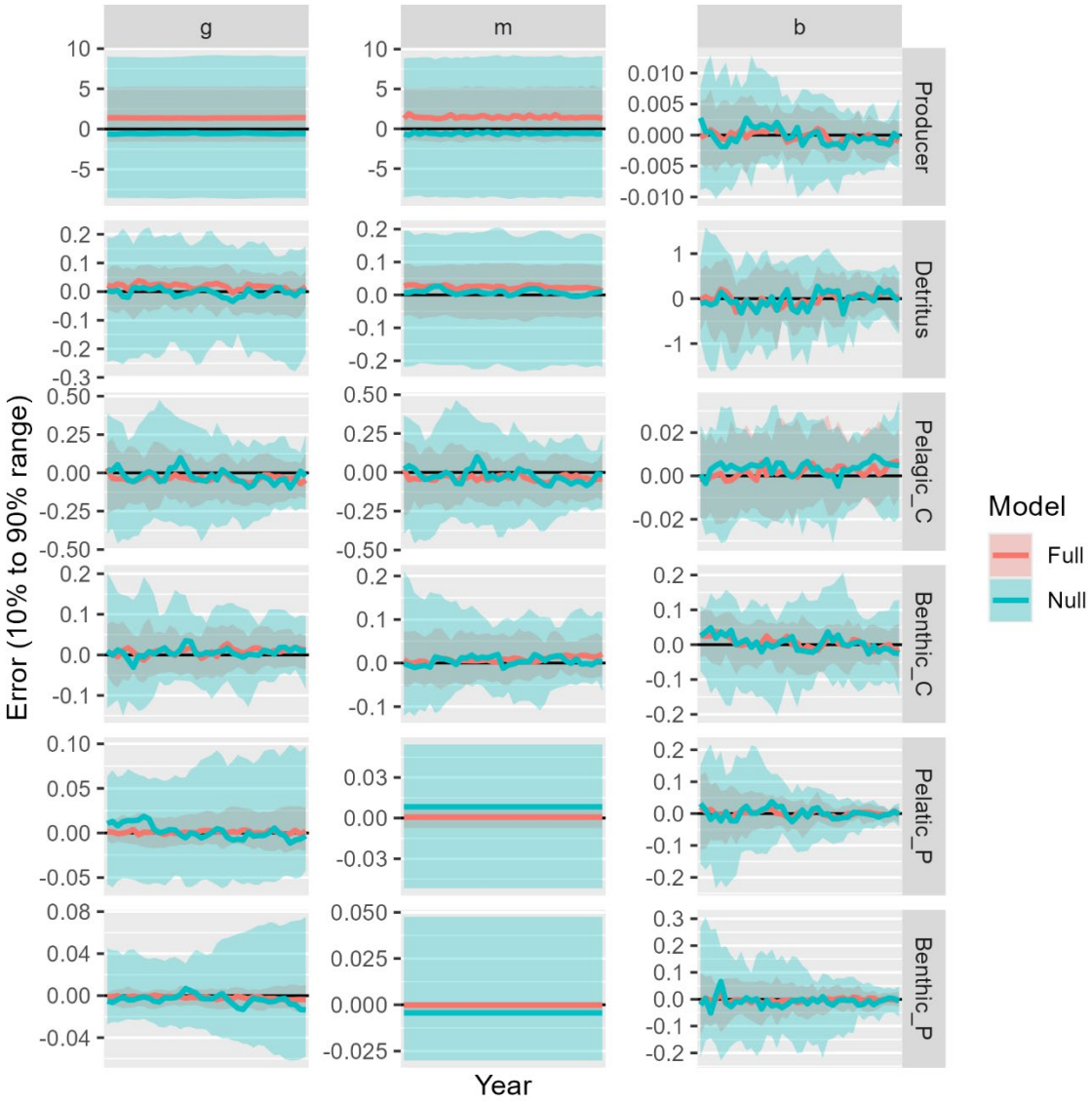

Fig. S6 -- Performance for estimated parameters in the simulation experiment (see Fig. S4 caption for details), showing the true value (red), and estimates from the full (green) or null model (blue) for each of 23 parameters when also estimating production per biomass p_s for all six taxa and consumption per biomass w_s for consumers and predators.